

**A MULTISTAGE CYCLONE ARRAY FOR THE COLLECTION OF SIZE-  
SEGREGATED SILICA AEROSOLS TO TEST THE HYPOTHESIS THAT  
ULTRAFINE CRYSTALLINE SILICA PARTICLES ARE MORE EFFICIENT IN  
THEIR ACTIVATION OF MACROPHAGES**

by

**Steven E. Mischler**

BA, Kenyon College, 1989

MS, University of Michigan, School of Public Health, 1991

Submitted to the Graduate Faculty of  
the Graduate School of Public Health in partial fulfillment  
of the requirements for the degree of  
Doctor of Philosophy

University of Pittsburgh

2013

UNIVERSITY OF PITTSBURGH  
GRADUATE SCHOOL OF PUBLIC HEALTH

This dissertation was presented

by

Steven E. Mischler

It was defended on

November 20, 2013

and approved by

Claudette M. St. Croix, PhD, Assistant Professor, Environmental and Occupational Health, Assistant Director, Center for Biologic Imaging, University of Pittsburgh

Bruce R. Pitt, PhD, Professor and Chairman, Department of Environmental and Occupational Health, Graduate School of Public Health, University of Pittsburgh

Hunter Champion, MD, PhD, FAHA, Associate Professor of Medicine  
Division of Pulmonary, Allergy and Critical Care Medicine, the Vascular Medicine  
Institute and the Cardiovascular Institute, University of Pittsburgh

**Dissertation Advisor:** Luis A. Ortiz, MD, PhD, Associate Professor, Department of  
Environmental and Occupational Health, Graduate School of Public Health,  
University of Pittsburgh

Copyright © by Steven E. Mischler

2013

**A MULTISTAGE CYCLONE ARRAY FOR THE COLLECTION OF SIZE-SEGREGATED SILICA AEROSOLS TO TEST THE HYPOTHESIS THAT ULTRAFINE CRYSTALLINE SILICA PARTICLES ARE MORE EFFICIENT IN THEIR ACTIVATION OF MACROPHAGES**

Steven E. Mischler, PhD

University of Pittsburgh, 2013

**ABSTRACT**

Occupational exposure to crystalline silica is a well-established occupational hazard. Once in the lung, crystalline silica particles can result in the activation of alveolar macrophages potentially leading to silicosis, a fibrotic lung disease. Because the activation of alveolar macrophages is the beginning step in a complicated inflammatory cascade, it is necessary to define the particle characteristics resulting in this activation. In this study a serial multi-cyclone sampling array (MCSA) capable of simultaneously sampling particles of multiple size fractions, from an occupational environment, was developed and tested and then used to collect size-segregated crystalline silica particles to determine the effect of the size of crystalline silica particles on the activation of macrophages. The MCSA method is an improvement over current methods used to size-segregate occupational aerosols for characterization, due to its simplicity and its ability to collect sufficient masses of nano- and ultrafine sized particles for analysis. This method was evaluated in a chamber providing a uniform atmosphere of dust concentrations using crystalline silica particles. The multi-cyclone sampling array was used to segregate crystalline silica particles into four size fractions, from a chamber concentration of  $10 \text{ mg/m}^3$ . The size distributions of the particles collected at each stage were confirmed, in the air, before and after each cyclone stage. Once collected, the particle size distribution of each size fraction was measured using light scattering techniques, to further confirm the size distributions. As a final

confirmation, scanning electron microscopy was used to collect images of each size fraction. The results presented here, using multiple measurement techniques, show that this multi-cyclone system was able to successfully collect distinct size-segregated particles at sufficient masses to perform toxicological evaluations and physical/chemical characterization.

Once the particles were collected using the MCSA they were used to determine the effect of the size of crystalline silica particles on the activation of macrophages. RAW 264.7 macrophages were exposed to four different sizes of crystalline silica and their activation was measured using electron microscopy, reactive oxygen species (ROS) generation by mitochondria, and cytokine expression. These data identified differences in particle uptake and formation of subcellular organelles based on particle size. In addition, these data show that the smallest particles, with a geometric mean of diameter 0.3  $\mu\text{m}$ , significantly increase the generation of mitochondrial ROS and the expression of cytokines when compared to larger crystalline silica particles, with a geometric mean diameter of 4.1  $\mu\text{m}$ .

With regard to occupational and public health significance, our data indicate the necessity of properly characterizing occupational aerosols using regulatory exposure metrics that are effectively protective against particle exposure causing adverse effects on workers' health.

## TABLE OF CONTENTS

ACKNOWLEDGEMENTS .....	x
1.0 INTRODUCTION .....	1
1.1 CS EXPOSURE .....	1
1.2 PARTICULATE MATTER REGULATION AND MEASUREMENT .....	2
1.3 DO SMALL PARTICLES EQUAL BIG PARTICLES .....	2
1.4 SMALL PARTICLES AND HEALTH EFFECTS MODELS .....	4
1.5 CURRENT SAMPLING METHODS TO SIZE-SEGREGATE OCCUPATIONAL AEROSOLS .....	6
1.6 CYCLONES AND SIZE-SELECTIVE SAMPLING.....	10
1.7 SCOPE OF DISSERTATION AND STATEMENT OF HYPOTHESIS.....	11
2.0 A MULTIC-CYCLONE SAMPLING ARRAY FOR THE COLLECTION OF SIZE- SEGREGATED OCCUPATIONAL AEROSOLS.....	13
2.1 ABSTRACT .....	14
2.2 INTRODUCTION.....	15
2.3 METHODS.....	17
2.4 RESULTS.....	20
2.5 DISCUSSION .....	34
2.6 CONCLUSION .....	37
3.0 DIFFERENTIAL ACTIVATION OF MURINE ALVEOLAR MACROPHAGES BY SIZE-SEGREGATED CRYSTALLINE SILICA .....	39
3.1 ABSTRACT .....	40
3.2 INTRODUCTION.....	41
3.3 METHODS.....	43
3.4 RESULTS.....	48
3.5 DISCUSSION .....	65
4.0 CONCLUSIONS.....	71
BIBLIOGRAPHY .....	77

## LIST OF TABLES

Table 1: Specifications for cyclones used in the multi-cyclone sampling array.....	26
Table 2: Mean particle diameter for each size range using DLS/LLS data. ....	31
Table 3: Mass of crystalline silica particles collected at each MCSA stage.....	34
Table 4: Mean particle diameter and standard deviation for each size range using DLS/LLS data. .....	49
Table 5: Grouping of Time Points for mROS statistical analysis.....	58
Table 6: Results of Independent Samples t-tests for mROS measurements. ....	59

## LIST OF FIGURES

Figure 1: Picture and schematic of low pressure cascade impactor.....	7
Figure 2: Versatile Aerosol Concentration Enrichment system (VACES) at the Office of Mine Safety and Health Laboratory. ....	9
Figure 3: Schematic showing parts and design of a cyclone. ....	11
Figure 4: Schematic of the multi-cyclone sampling array and experimental design to confirm particle separation. ....	21
Figure 5: Marple chamber at the Office of Mine Safety and Health laboratory.....	24
Figure 6: Aerosol penetration curve for each sampling stage calculated using AF.....	27
Figure 7: Size distribution of crystalline silica base material measured in the airstream (dotted line – SMPS, tan line-APS, solid black line – merged data). ....	28
Figure 8A: Size distribution of coarse particles collected by HD cyclone (dotted line). These data were calculated from SMPS/APS measurements of the airstream before (black line) and after (square markers) the HD cyclone. ....	29
Figure 8B: Size distribution of respirable particles collected by SCC 2.2 cyclone (dotted line). These data were calculated from SMPS/APS measurements of the airstream after the HD cyclone (black line) and after the SCC 2.2 (square marker).....	29
Figure 8C: Size distribution of submicron and ultrafine particles collected by SCC 4.4 cyclone (gray-dotted line) and filter (square marker), respectively. These data were calculated from SMPS/APS measurements of the airstream after the SCC 2.2 (black line) and after the SCC 4.4 (square markers).....	30

Figure 9: Size distribution of crystalline particles from each stage of the MCSA method, calculated from light scattering data. ....	31
Figure 10: SEM photographs at 5,000 magnification of crystalline silica particles retrieved from Higgins Dewell cyclone: (coarse) (A), SCC 2.2 (respirable) (B), SCC 4.4 (submicron) (C), and Filter (ultrafine) (D). ....	33
Figure 11: SEM photographs at 5,000 magnification of crystalline silica particles used for this study: A) Ultrafine (UF), B) Submicron (S), C) Respirable (R), and D) Coarse (C). ....	50
Figure 12: TEM images after 1-hour exposure of AM to Coarse and UF particles. ....	52
Figure 13: High Magnification (20,000X) TEM image at AM exposed to UF particles for 1 hour. ....	53
Figure 14: TEM images after 2-hour exposure of AM to Coarse and UF particles. ....	54
Figure 15: High Magnification (20,000X) TEM image of AM exposed to UF particles for 2 hours. ....	55
Figure 16: TEM images after 4-hour exposure of AM to Coarse and UF particles. ....	56
Figure 17: High Magnification (15,000X) TEM image of AM exposed to UF particles for 4 hours. ....	57
Figure 18A: Representative images of the live cell experiment collected at 0, 1, 2 and 3 hours.	60
Figure 18B: Increase in fluorescence over background resulting from exposure of RAW 264.7 cells to UF and C particles. ....	61
Figure 19A: TNF- $\alpha$ expression after 2-hour exposure to four sizes of Crystalline Silica. ....	63
Figure 19B: TNF- $\alpha$ expression after 4-hour exposure to four sizes of Crystalline Silica. ....	64
Figure 19C: TNF- $\alpha$ expression after 8-hour exposure to four sizes of Crystalline Silica. ....	65

## ACKNOWLEDGEMENTS

I express deep gratitude to Dr. Luis Ortiz and Dr. Claudette M. St. Croix without whom this dissertation could not have been achieved. In addition I would like to thank Dr. Michelangelo Di Giuseppe and Dr. Emanuele Cauda for their assistance with this work. Each of their guidance, commitment, and patience were necessary to the understanding of the science and in the writing of the dissertation. Beyond professional gratitude, I would like to thank them for their personal kindness. I am in their debt.

I would also like to thank the rest of my committee members, Drs. Bruce Pitt, and Hunter Champion for making time in their schedules and for their suggestions and criticisms that improved my scientific proficiency.

Finally I would also like to express gratitude to my true champions who have followed my work from the beginning, my darling wife, Shannon J. Mischler and children, William, Peter and Eva. Their love, support and understanding during this decade of study, allowed me to persevere, and charge ahead when times were dark, bringing me nutritional laughter, hugs and smiles when they were needed most. We did it!

## **1.0 INTRODUCTION**

### **1.1 CS EXPOSURE**

Occupational exposure to crystalline silica (CS) affects at least 1.7 million US workers (NIOSH, 2002) and is associated with the development of silicosis, a fibrotic lung disease which is one of the most important occupational diseases worldwide (Greenberg et al., 2007, WHO, 2007, Leung et al., 2012). The National Institute for Occupational Safety and Health reported that 300 silicosis-related deaths occurred each year in the United States between 1991 and 1995 (NIOSH, 2013). During those same years China recorded 24,000 silicosis-related deaths per year (WHO, 2000). These numbers indicate that silicosis remains a fundamental occupational exposure problem in both the developing and developed countries (Huaux, 2007).

Exposure to CS occurs in many occupations and industries. The United States Occupational Safety and Health administration (OSHA) measured detectable levels of respirable CS in samples collected in 255 different industries (NIOSH, 2002). In general, silica exposure will occur in any occupation which includes grinding or mechanically breaking material containing silica (mining, construction) or handling fine particles containing silica, such as silica sand (fracking) (Sirianni et al., 2008, Leung et al., 2012, Beaudry et al., 2013, Hall et al., 2013, McKinney et al., 2013, Sauve et al., 2013).

## **1.2 PARTICULATE MATTER REGULATION AND MEASUREMENT**

Currently, the exposure to aerosols, such as CS, in the ambient air or the workplace is expressed on a mass per unit volume basis. For example, the US EPA set the annual ambient air quality standard for PM<sub>2.5</sub> (particulate matter with an aerodynamic diameter < 2.5 μm) at 15 μg/m<sup>3</sup> (40 CFR Part 50). The Mine Safety and Health Administration (MSHA) requires that the average concentration of respirable dust in underground coal mines remains below 2 mg/m<sup>3</sup> over the entire working shift (30 CFR Part 70). The use of the mass based metric became popular because mass was an easy metric to measure and potential health impacts were well correlated with mass of inhaled material (Maynard and Aitken, 2007).

Epidemiologic studies support the use of a mass metric. Several groups published papers showing that elevated ambient fine particulate pollution (PM<sub>2.5</sub>) was associated with increased risk of acute ischemic coronary events (Brook et al., 2010, Pope et al., 2006). The National Morbidity, Mortality and Air Pollution Study (NMMAPS) reported a positive association between PM<sub>10</sub> (particulate matter with an aerodynamic diameter < 10 μm) and death (Sarnat et al., 2000). Also, Silverman (Silverman et al., 2012) recently reported a significant increase in lung cancer risk was associated with exposure to increasing mass concentrations of respirable elemental carbon in underground miners.

## **1.3 DO SMALL PARTICLES EQUAL BIG PARTICLES**

With the advent of the field of nanotechnology it has become necessary to more fully define a particle's characteristics to understand its potential toxicology (Murdock et al., 2008).

Because smaller particles have a higher surface area per unit mass when compared to larger particles, smaller particles may more readily start potential negative biological reactions, such as inflammation (Monteiller et al., 2007). In current regulation, nano-sized material is typically treated as a variation of the base material, with similar hazards. However, the conversion of a base material to a nano-sized particle can impart new properties with resulting new toxicology (Oberdorster et al., 2005). This different toxicology may result because particle size is a determinant on where in the respiratory tract the particle deposits (Maynard and Aitken, 2007, Paur et al., 2011), as well as the physicochemical characteristics, including size distribution, particle morphology, reactivity and surface chemistry, of the smaller particles (Wittmaack, 2011, Maynard and Aitken, 2007). Because the biological effects cannot simply be extrapolated based on the physical/chemical properties of bulk material alone, experimental determination of these effects as a function of particle size is necessary for advancing the science on the toxicity of these particles (Waters et al., 2009).

The above discussion suggests that a mass metric may not fully indicate the potential toxicity of ultrafine and nano-particles. At particle concentrations in air below established mass-based exposure levels, very high particle number concentrations - up to  $10^6 \text{ cm}^{-3}$  in occupational environments and  $10^4 \text{ cm}^{-3}$  in ambient air - exist (Bugarski et al., 2009, Hughes LS, 1998) , and this high number concentration is likely to result in toxicological effects, even at low ambient mass concentrations (Oberdorster et al., 2005). Thus exposure to ultrafine and nano-particles presents the potential for the occupational exposure to these particles to be below the mass-based regulatory levels yet still result in negative health effects in the exposed worker.

Occupational exposure to crystalline silica is a good example of this possibility because although the mortality attributable to crystalline silica exposure steadily decreased beginning in 1970, with the introduction of national mass-based compliance standards, the death rate from silicosis has remained constant since 2000 and workers exposed (the Centers for Disease Control and Prevention estimates over 2 million people every year in the US) to silica below permissible and recommended exposure limits are still at risk for developing silicosis (Centers for Disease and Prevention, 2005, National Institute for Occupational Safety and Health, 2002). These data identify a potential breach in the effectiveness of mass-based primary prevention standards in reducing mortality and suggest that further adjustments in the regulations may be required to eliminate silica-induced mortality. Although occupational exposure to CS and the related health effects have been well documented in the scientific literature, many uncertainties still exist including the effect of the crystals surface characteristics, including particle size, on the development of disease (Wiessner et al., 1989, Fubini and Hubbard, 2003, Bodo et al., 2007, Kajiwara et al., 2007, Wang et al., 2007, Sirianni et al., 2008, Leclerc et al., 2012).

#### **1.4 SMALL PARTICLES AND HEALTH EFFECTS MODELS**

Most atmospheric studies suggest that the concentration of smaller particles correlate better with adverse health effects than the concentration of larger particles (Churg and Brauer, 2000, Donaldson and MacNee, 2001, Kajiwara et al., 2007, Knol et al., 2009, Pope et al., 2009). Because smaller particles have a higher surface area per unit mass when compared to larger particles, smaller particles may more readily start potential negative biological reactions, such as inflammation (Monteiller et al., 2007). Chronic inflammation has been implicated in the

pathogenesis of silicosis. In this scenario, the immune cells (alveolar macrophages, epithelial cells and fibroblasts) are activated and release a host of inflammatory cytokines and generate reactive oxygen species (ROS) resulting in the recruitment of additional inflammatory cells, predominantly alveolar macrophages. The influx of additional inflammatory cells and release of ROS damages pulmonary architecture causing accumulation of connective tissue products (Mossman and Churg, 1998, Fubini and Hubbard, 2003, Rimal et al., 2005, Huaux, 2007, Hamilton et al., 2008). Knowledge of the degree to which particle size effects the activation of macrophages and the resulting ROS generation and inflammatory response is necessary for fully elucidating the mechanisms leading to silicosis from occupational exposure to CS. Several groups have studied the pathways leading from the phagocytosis of occupational aerosols, including CS, by alveolar macrophages to the inflammatory response including the expression of ROS and cytokines (Fubini and Hubbard, 2003, Li et al., 2003, Balduzzi et al., 2004, Hamilton et al., 2008, Cox, 2011). However, even though tremendous advancements in describing these pathways the underlying mechanisms are still poorly defined (Stern et al., 2012). The basic model, specifically for CS, as outlined by Hamilton (Hamilton et al., 2008) and refined by Cox (Cox, 2011), begins with the engulfment of the CS particle by the macrophage. Upon internalization the phagosome combines with a lysosome to form a phagolysosome. At this stage the CS particles react with the phagolysosomal membrane, resulting in membrane permeabilization. This loss of lysosome membrane integrity is induced by the acidic phagolysosome environment, cathepsin D activity and acidic sphingomyelinase activity (Thibodeau et al., 2004, Kroemer and Jaattela, 2005), and results in the release of cathepsins and other catabolic hydrolases, and ROS (Stern et al., 2012). This lysosomal release then causes mitochondrial outer membrane permeabilization resulting in the generation of mitochondrial

ROS. The elevated ROS environment will lead to the secretion of pro-inflammatory mediators, including TNF- $\alpha$ , as well as growth factors important in lung fibrosis (Cox, 2011).

As discussed earlier, previous research suggests that exposure to smaller particles correlate better with adverse health effects than exposure to larger particles. One way to test this hypothesis, using the model proposed above for CS, is to expose alveolar macrophages to different sized CS particles and measure their activation using endpoints in the described models, such as formation of phagolysosomes, generation of mitochondrial ROS and expression of pro-inflammatory mediators. Results from these experiments would help to elucidate some of the uncertainties that still exist regarding the effects of particle size on the development of disease.

## **1.5 CURRENT SAMPLING METHODS TO SIZE-SEGREGATE OCCUPATIONAL AEROSOLS**

Currently, there is very little published data on the size dependent toxicity of airborne particulates, such as crystalline silica (Ramgolam et al., 2009, Ruusunen et al., 2011). One difficulty in completing size-dependent toxicity studies with CS, or other occupational aerosols, is the difficulty in separating these aerosols into distinct size ranges and in necessary quantities for toxicological studies while avoiding sampling error (Stephanie et al., 2011). In the last few years, research groups have published data on two systems to collect samples for size-selective toxicity sampling. One of these systems is a 13-stage low pressure cascade impactor (Figure 1). Ramgolam (Ramgolam et al., 2009) and Stephanie (Stephanie, 2011) collected ambient aerosols and used this impactor to partition the ambient aerosols into distinct size classes. In these studies, the aerosols were collected onto a polycarbonate collection substrate. This substrate was then

weighed to determine the amount of mass collected at each stage and then the substrates were sonicated in culture media to remove the aerosols. The substrates were then examined, via scanning electron microscopy, to ensure the particles were removed. The in-vitro tests were then performed using the media from the sonication step.

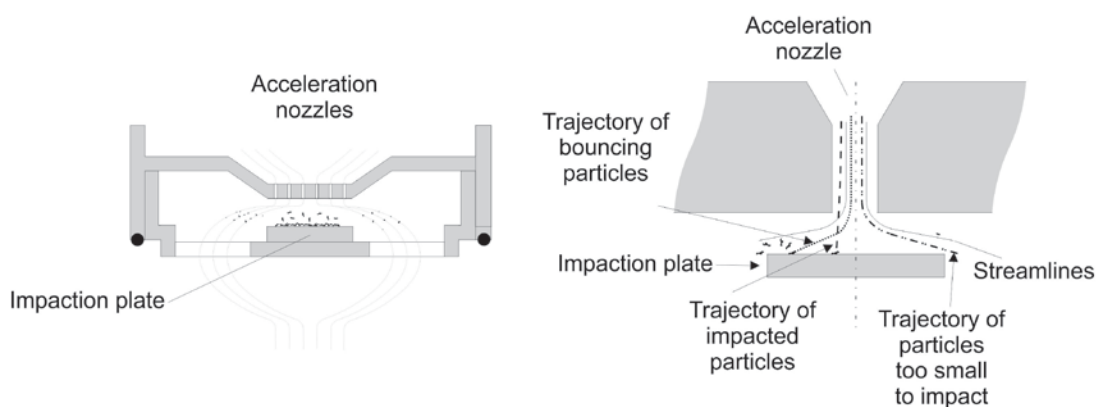


**Figure 1: Picture and schematic of low pressure cascade impactor.**

This collection system has drawbacks when used to collect particles for toxicity testing. The first drawback, and one that has serious consequences when using this sampler for toxicological studies is the efficiency with which particles of different sizes are collected during the impaction process (Virtanen et al., 2010). When attempting to sample particles at masses necessary for toxicological tests overloading can occur. Overloading is a process where layers of previously collected particles result in a change of particle size collected at each stage, through particle bounce or de-agglomeration (Vanderpool et al., 2001). Substrate overloading results in larger particles being collected on substrates for smaller particles, and given the relative masses between large and small particles, this unintended intrusion of large particles on small particle

substrates could result in a positive bias towards mass of small particles (Kenny et al., 2000). When these overloaded substrates are then used for toxicological tests, the cells may be exposed to particles which are larger than intended. A second drawback is that this method is extremely labor intensive. For each sampling scenario it is necessary to weight and then load substrates into all 13 stages of this device. After sampling, it is again necessary to remove substrates from each stage, weight the substrate and then clean each stage. Once the substrates are removed they must be sonicated to extract the particles. A third drawback is the handling of the particles during both the impaction and sonication steps. In general, the fewer steps involved between removing the aerosols from the atmosphere and exposing the cells, the lower the possibility of changing the physical property of the aerosols. As noted above, changing the physical properties of the aerosols could result in a change in their biological effect.

A second methodology used to collect particles for in vitro toxicity testing is a Versatile Aerosol Concentration Enrichment system (VACES). This system is described in detail by Kim et.al. (Kim et al., 2001b). This system segregates particles into three size fractions, ultrafine ( $<0.1\mu\text{m}$ ); accumulation (between  $0.1$  and  $2.5\mu\text{m}$ ) and coarse ( $2.5 - 10\mu\text{m}$ ) and collects these particles using a liquid impinger. In research (unpublished) at the Office of Mine Safety and Health Research (OMSHR), we have found two drawbacks of this system: 1) the system is large and complicated making it impractical for field evaluations (Figure 2), and 2) the VACES collection system is inefficient when collecting smaller particles, resulting in a higher percentage of larger particles in each size range being collected and making it difficult to calculate the precise amount of mass collected into each impinger liquid. Since the impinger liquid is then used to expose cells, this system skews the size distribution towards larger particles and does not allow for an exact calculation of the exposure mass at each size fraction.

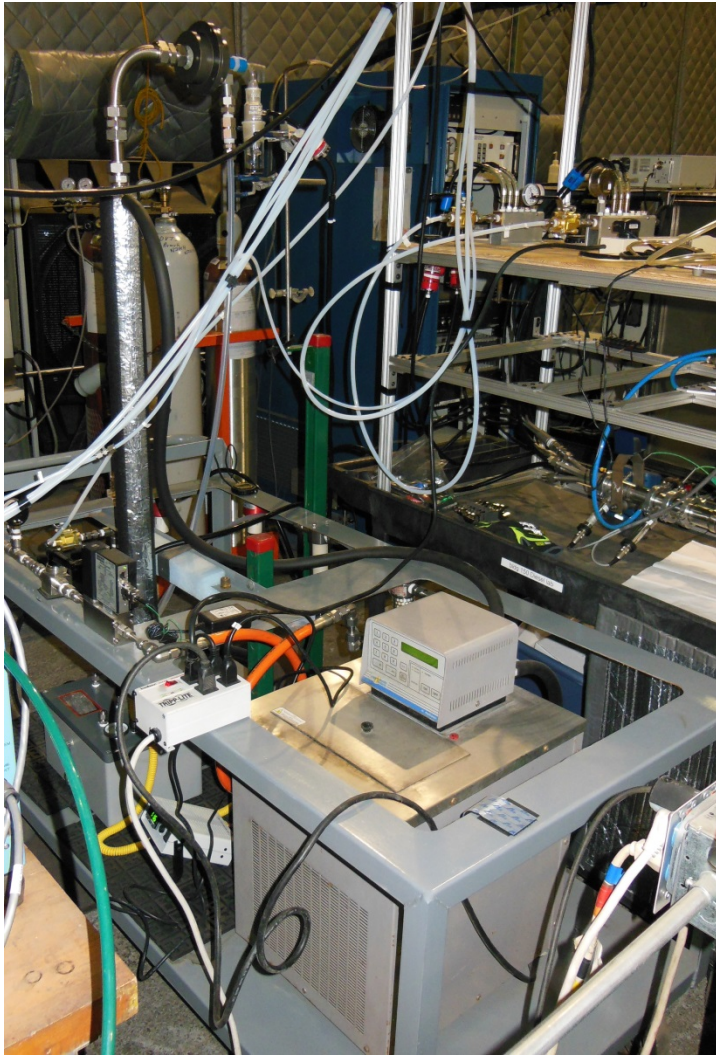


**Figure 2: Versatile Aerosol Concentration Enrichment system (VACES) at the Office of Mine Safety and Health Laboratory.**

Steenhof (Steenhof et al., 2011) used this system to evaluate in vitro toxicity associated with size fraction. A conclusion from this study was that insufficient mass was collected to perform toxicity studies at the desired concentrations.

## 1.6 CYCLONES AND SIZE-SELECTIVE SAMPLING

The loading effects noted for the impactor precludes its use for collection of a large mass of size-segregated particles. However, cyclonic devices were demonstrated to have significant advantages over impactors for extended operation and high mass loadings (Kenny et al., 2004).

Cyclones have also been widely used for size-selective particle sampling. Cyclones offer a suitable alternative to impactors if they supply a similar size cut point, sharpness and mass penetration. A cyclone consists of three basic parts, an upper cylindrical barrel, a lower cone, and a grit pot (Figure 3). Air enters tangentially into the barrel and travels downward into the cone with increasing air velocity. This increasing air velocity results in centrifugal forces which separate the particles from the air stream. Once at the bottom of the cone the air stream changes direction and moves vertically out of the cyclone while the trapped particles slide into the grit pot from which the particles can be easily removed after the completion of sampling. Typically, cyclones can be designed for applications needing a specific  $d_{50}$  (particle aerodynamic diameter with 50% penetration efficiency through the cyclone) and sharpness using the cyclone's body dimensions and flow rate through the cyclone (Kenny and Gussman, 1997). Kenny (Kenny et al., 2000) concluded that cyclones can be designed to provide a sufficiently sharp cut for ambient monitoring applications. In addition, Kenny's research showed that impactors loaded with < 3 mg of dust resulted in deterioration in the impactors' performance.

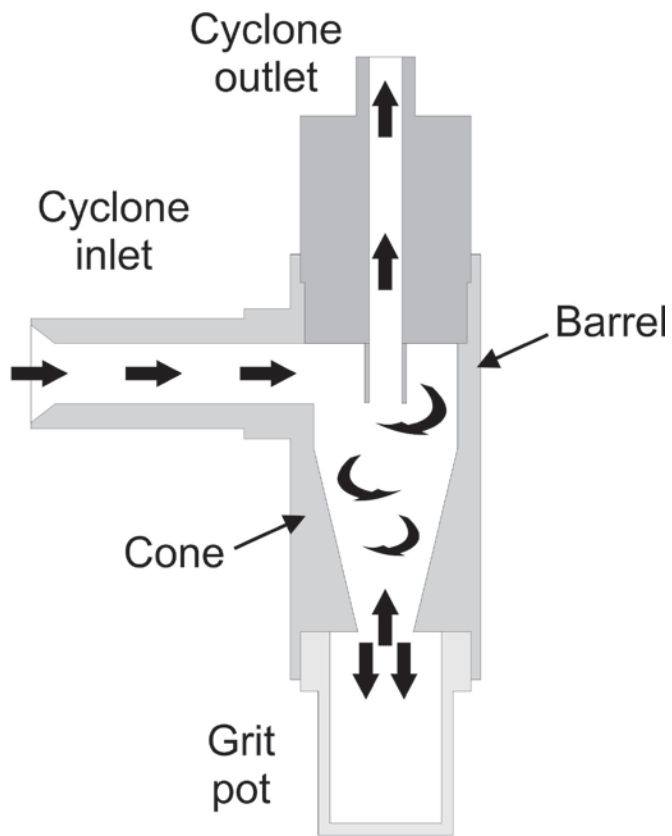


**Figure 3: Schematic showing parts and design of a cyclone.**

## **1.7 SCOPE OF DISSERTATION AND STATEMENT OF HYPOTHESIS**

Based on the premise that the current sampling methods are not capable of providing size-segregated occupational aerosols in necessary quantities for toxicological studies, while avoiding sampling error, a multi-cyclone sampling array (MCSA) method is proposed. The first hypothesis of this current research is that cyclones can be used in this method to 1) successfully separate a standard occupational aerosol into distinct size fractions, 2) enable recovery of these

aerosols, with minimal handling steps, in a form appropriate for use in toxicity experiments, and 3) enable collection of an appropriate mass of each size class of aerosols to perform the toxicity tests. Chapter 2 provides the results from this first hypothesis.

Once this sampling method was designed and evaluated, it was possible to test our second hypothesis that smaller crystalline silica particles will enhance the activation of alveolar macrophages resulting in an enhanced inflammatory response. This hypothesis was tested by exposing RAW 264.7 macrophages to four different sizes of crystalline silica, collected using the MCSA, and their activation was evaluated using electron microscopy, reactive oxygen species generation by the mitochondria and cytokine expression (chapter 3).

## **2.0 A MULTIC-CYCLONE SAMPLING ARRAY FOR THE COLLECTION OF SIZE-SEGREGATED OCCUPATIONAL AEROSOLS**

Steven E. Mischler<sup>1</sup>, Emanuele G. Cauda<sup>1</sup>, Michelangelo Di Giuseppe<sup>2</sup>, and Luis A. Ortiz<sup>2</sup>

<sup>1</sup> National Institute for Occupational Safety and Health, Office of Mine Safety and Health  
Research, Pittsburgh, Pennsylvania

<sup>2</sup> University of Pittsburgh, Department of Environmental and Occupational Health, Pittsburgh,  
Pennsylvania

**Adapted from publication (Mischler et al., 2013) in Journal of Occupational and  
Environmental Hygiene**

## 2.1 ABSTRACT

In this study a serial multi-cyclone sampling array capable of simultaneously sampling particles of multiple size fractions, from an occupational environment, for use in *in vivo* and *in vitro* toxicity studies and physical/chemical characterization, was developed and tested. This method is an improvement over current methods used to size-segregate occupational aerosols for characterization, due to its simplicity and its ability to collect sufficient masses of nano- and ultrafine sized particles for analysis. This method was evaluated in a chamber providing a uniform atmosphere of dust concentrations using crystalline silica particles. The multi-cyclone sampling array was used to segregate crystalline silica particles into four size fractions, from a chamber concentration of 10 mg/m<sup>3</sup>. The size distributions of the particles collected at each stage were confirmed, in the air, before and after each cyclone stage. Once collected, the particle size distribution of each size fraction was measured using light scattering techniques, to further confirm the size distributions. As a final confirmation, scanning electron microscopy was used to collect images of each size fraction. The results presented here, using multiple measurement techniques, show that this multi-cyclone system was able to successfully collect distinct size-segregated particles at sufficient masses to perform toxicological evaluations and physical/chemical characterization.

## 2.2 INTRODUCTION

The exposure to aerosols in the workplace is generally measured on a mass per unit volume basis. For example, the Occupational Safety and Health Administration (OSHA) regulates the concentration of inert or nuisance particulates in the construction industry with a threshold limit value (TLV) of 15 mg/m<sup>3</sup>(<sup>29 CFR Part 1926 Subpart D</sup>). The Mine Safety and Health Administration (MSHA) requires that the average concentration of respirable dust in underground coal mines remains below 2 mg/m<sup>3</sup> over the entire working shift (30 CFR Part 70). The use of the mass based metric became popular because mass was an easy metric to measure and observed health outcomes were well correlated with mass of inhaled material (Maynard and Aitken, 2007, Brook et al., 2010, Pope et al., 2006, Sarnat et al., 2000, Silverman et al., 2012).

With the advent of the field of nanotechnology and the potential for workers to be exposed to smaller and smaller particles, it has become increasingly necessary to more fully define a particle's characteristics to understand its potential toxicology because smaller particles have a higher number concentration and surface area per unit mass when compared to larger particles. (Murdock et al., 2008, Monteiller et al., 2007). Oberdorster et al. (Oberdorster et al., 2005) reported that a decrease in particle size is associated with a significant increase in particle number and surface area. In current regulation, nano-sized material is typically treated as a variation of the base material, with similar hazards. However, the conversion of a base material to a nano-sized particle can impart new properties with resulting new toxicology (Oberdorster et al., 2005). This different toxicology may result because particle size is a determinant on where in the respiratory tract the particle deposits (Maynard and Aitken, 2007, Paur et al., 2011), as well as the physicochemical characteristics, including size distribution, particle morphology,

reactivity and surface chemistry, of the smaller particles (Wittmaack, 2011, Maynard and Aitken, 2007, Monteiller et al., 2007, Stephanie et al., 2011). Because the biological effects cannot simply be extrapolated based on the physical/chemical properties of bulk material alone, experimental determination of these effects as a function of airborne particle size is necessary for advancing the science on the toxicity of these particles (Waters et al., 2009).

The above discussion suggests that a mass metric may not fully indicate the potential toxicity of ultrafine and nano-particles. At particle concentrations in air below established mass-based exposure levels, very high particle number concentrations - up to  $10^6 \text{ cm}^{-3}$  in occupational environments and  $10^4 \text{ cm}^{-3}$  in ambient air - exist (Bugarski et al., 2009, Hughes LS, 1998) , and this high number concentration is likely to result in toxicological effects, even at low ambient mass concentrations (Oberdorster et al., 2005). Thus exposure to ultrafine and nano-particles presents the potential for the occupational exposure to these particles to be below the mass-based regulatory levels yet still result in negative health effects in the exposed worker.

Occupational exposure to crystalline silica is a good example of this possibility. Although the mortality attributable to crystalline silica exposure steadily decreased beginning in 1970, with the introduction of national mass-based compliance standards, the death rate from silicosis has remained constant since 2000 (Centers for Disease and Prevention, 2005). In addition, workers exposed to silica below permissible and recommended exposure limits are still at risk for developing silicosis (Centers for Disease and Prevention, 2005, National Institute for Occupational Safety and Health, 2002). These data identify a potential breach in the effectiveness of mass-based primary prevention standards in reducing mortality and suggest that further adjustments in the regulations may be required to eliminate silica-induced mortality.

Currently, there is very little published data on the size dependent toxicity of airborne particulates, such as crystalline silica (Ramgolam et al., 2009, Ruusunen et al., 2011). One possible reason for this fact is the lack of a standardized, feasible sampling/recovery method for size-based sampling of occupational or ambient aerosols that allows for collection of sufficient material while avoiding sampling error (Stephanie et al., 2011).

The purpose of this study is to develop and bench-test a multi-cyclone sampling array (MCSA) capable of simultaneously sampling particles of multiple size fractions for use in toxicological studies or physical and chemical analysis. This paper focuses on the description of the MCSA method and the assessment, in the laboratory, of its ability to 1) successfully separate a standard occupational aerosol into distinct size fractions, 2) enable recovery of these distinct size fractions, with minimal handling steps, in a form appropriate for use in characterization experiments, and 3) enable collection of an appropriate mass of each size class of aerosols to perform the characterization testing.

## 2.3 METHODS

**Cyclones:** For this research two cyclone designs were used. A Higgins Dewell (HD) cyclone (BGI Inc., Waltham, MA) and a newly designed Sharp Cut cyclone (SCC) also made by BGI Incorporated. The HD was designed to achieve a  $d_{50}$  of 4.0  $\mu\text{m}$  at a flow rate of 2.2 liters per minute (lpm) and the SCC was designed to achieve a  $d_{50}$  of 0.8  $\mu\text{m}$  at a flow rate of 2.2 lpm.

**Particles used for method evaluation:** The crystalline silica ( $\text{SiO}_2$  quartz, 99.9%, 1 $\mu\text{m}$ , Stock #: 4807YL) used in this study was purchased from Nanostructured & Amorphous

Materials, Inc. (Houston, TX). Before particles were used in the experiment they were baked at 220°C for 24 hours to destroy potential contaminating endotoxins.

**Confirmation of Size Distribution of Airborne Particles:** The size distribution of the airborne crystalline silica, both before and after each cyclone stage, was measured using both aerodynamic particle sizer (APS)(TSI, 2012a) and a scanning mobility particle sizer (SMPS)(TSI, 2012b) measurements. The APS was used for particles with aerodynamic diameters from 0.5 to 20 microns, whereas the SMPS was used for electromobility measurements of particles ranging from 0.025 to 0.6 microns. The electromobility size distribution measured by the SMPS was converted to aerodynamic size distribution by assuming a density of 2.6 g/cm<sup>3</sup> for the silica particles. The data from these two instruments were merged using TSI software. The size distribution of particles collected at each cyclone stage was calculated, using APS and SMPS measurements, by subtracting the size distribution of the particles measured after the cyclone stage from the size distribution of particles measured before each cyclone stage.

**Confirmation of Size Distribution of Collected Particles:** Two light scattering techniques were used to confirm the size distribution of the particles collected from each stage of the MCSA. Dynamic light scattering (DLS) is a broadly used and widely accepted method for measuring particle size in solution (Pristinski and Chastek, 2009). DLS was used in this experiment to confirm the size of the particles in both the submicron and ultrafine ranges. For this technique the particles were mixed in ultrapure, deionized water. The DLS technique reported a geometric mean and standard deviation(Thomas, 1987) for both size ranges. The

particle size distribution was calculated using a normal distribution function from the measured mean and standard deviation. For the coarse and respirable particles, the distribution was directly measured using a laser light scattering (LLS) technique (Micromeritics Analytical Services, Norcross, GA). The DLS/LLS data is reported on a percent volume basis, whereas the SMPS/APS data is reported on a number concentration basis. In general the percent volume basis will result in a shift of the distribution to the right.

**SEM images of Collected Particles:** For a visual confirmation of the different-sized particles and to confirm their crystalline structure, images of particles collected at each cyclone stage were collected using a JEOL 6400 scanning electron microscope (SEM) (Peabody, MA). SEM images for each particle size were collected at 6000, 10,000, 20,000 and 100,000 times magnification. For SEM analysis the particles were mixed in ultrapure, deionized water and the water particle mixture was then filtered through a polycarbonate membrane filter with a 0.2  $\mu\text{m}$  pore size. The filter was dried and then coated with an ultrathin coating of electrically conducting material to enhance the SEM analysis. An energy dispersive electron spectrometer (EDS) was used with the SEM for elemental identification of the collected particles.

**Mass Measurements of Collected Particles:** Gravimetric determinations of the mass of particles collected at each cyclone stage and on the filter were completed on a Mettler-Toledo UMT2 microbalance, in a controlled environment (Page and Volkwein, 2009) of  $22.8 \pm 0.4^\circ\text{C}$  ( $73 \pm 0.7^\circ\text{F}$ ) and 50.2% relative humidity. Balance precision was greater than 5  $\mu\text{g}$  with a limit of quantitation of 14  $\mu\text{g}$ .

## 2.4 RESULTS

**Multi-Cyclone Sampling Array Description:** A schematic showing the MCSA is presented in Figure 4. The MCSA incorporates cyclones in a series of three successive stages. Each cyclone stage is used to capture a specific size range of particles, in decreasing sizes with each stage in the series. The innovative idea in this design is to use the particles collected in the cone and grit pot of each cyclone for characterization and analysis. In this method, three cyclone stages and one filter stage (after the final cyclone) were used to collect size-segregated crystalline silica particles. The exhaust from one cyclone was connected to the inlet of the next cyclone in the series using conductive tubing.

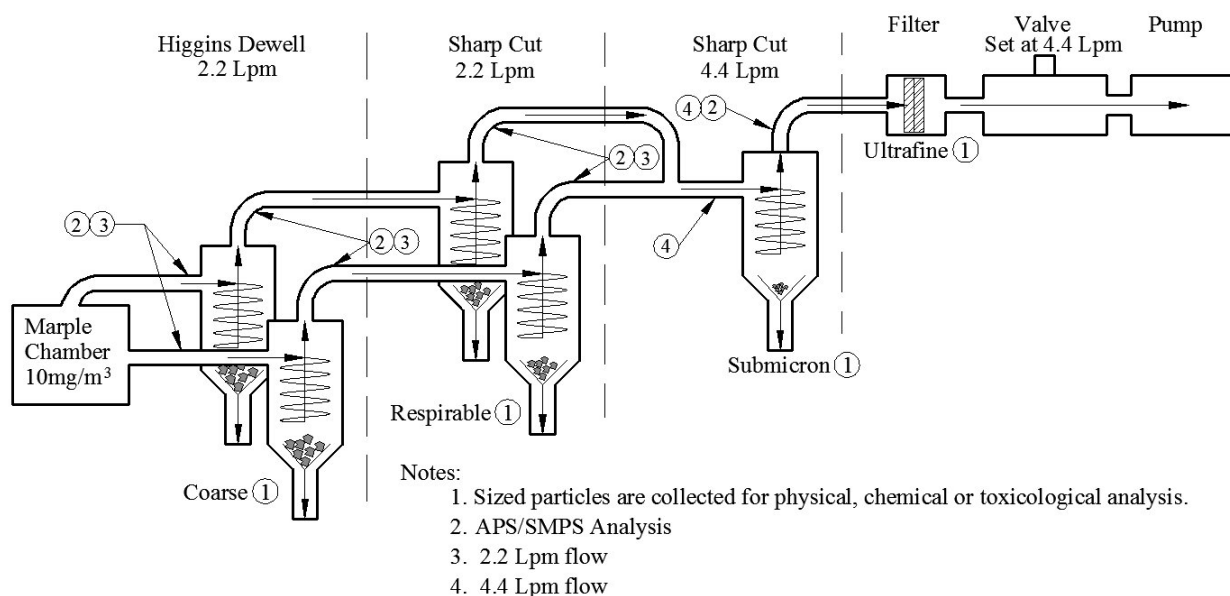


**Figure 4: Schematic of the multi-cyclone sampling array and experimental design to confirm particle separation.**

The first collection stage consisted of two HD cyclones in parallel with each cyclone receiving 2.2 lpm of particle laden air. Particles collected by these cyclones were labeled as coarse particles. The airstreams exiting the two HD cyclones, containing particles not collected by these cyclones, moved from the HD cyclone exhaust into the inlet of the cyclones in the second stage. This stage consisted of two SCC cyclones also running in parallel with each cyclone receiving 2.2 lpm of air. Particles collected by these cyclones were labeled as respirable particles. The exhaust from this stage, containing particles not collected by the first or second stage of cyclones, is then merged together, creating a combined flow rate of 4.4 lpm, and channeled to the inlet of a single sharp cut cyclone. This final cyclone stage consisted of a SCC flowing at 4.4 lpm. The  $d_{50}$  of the SCC flowing at 4.4 lpm was measured to be  $0.38\mu\text{m}$ . Particles collected by this stage were labeled as submicron. The exhaust from this final cyclone stage, containing particles not removed by the previous three cyclone stages was filtered by a 37 mm

polycarbonate membrane filter and the particles collected here were labeled as ultrafine particles. This is the only filter in the MCSA. Having only a single filter in this system significantly simplifies the system in regards to handling and particle extraction. Flow rates through each MCSA were kept constant with an in-line valve, plumbed into the system after the final filter, and measured at the HD cyclones before and after each sampling run. By merging the flows after the second cyclone stage (Figure 4), this method enables a further separation of the smallest particles into two size ranges (submicron and ultrafine). In addition these two final stages collect the smallest particles at an increased flow rate, which results in a larger air volume sampled and particle mass collected over the same time period and enhances the ability to quantitate the collected mass of these smallest particles.

**Particle Extraction from MCSA:** The size-segregated particles were collected from the grit pot of each cyclone using the following procedure. The grit pot was first inverted and tapped on the outside, allowing the particles to fall out of the grit pot and be collected onto an aluminum collection disk. Any particles which did not fall from the grit pot or particles which remained in the cone were scrapped from these surfaces using a plastic or wooden scrapping tool. Complete recovery of the particles from each cyclone was not important, only that the particles could be collected in sufficient mass, at each stage, for further characterization and analysis. Once the particles were fully recovered from each cyclone the particles were weighed and stored for later characterization and testing.

The pre-weighed filter, containing the smallest size range of particles, was post-weighed to determine the mass of particles collected on the filter. The particles collected on the filter were then removed by sonicating the filter in ultrapure, deionized water. The filter was then removed

from the solution, dried and reweighed to determine the mass of the particles removed from the filter. The extracted particles remained in solution. The removal efficiency was calculated by dividing the mass of particles remaining on the filter after extraction by the mass of particles on the filter before extraction.

Once separated and collected, the particles in each size range can be used for additional characterization and testing.

**Cutpoint Calculations for each Cyclone Stage:** An important step in the design process for the MCSA included selecting cyclones that would provide cutpoints to separate the particles into the desired size ranges. A key flexibility of this method is the ability to include cyclones designed to collect desired particle size ranges.

A detailed description of the method used to calculate the cyclones cutpoint is available in Maynard, 1995 (Maynard and Kenny, 1995). Briefly, the penetration efficiency of the SCC at each flow rate was characterized using ammonium fluorescein (AF) polydisperse aerosols in a calm air chamber. Aerosol characteristics were determined using the 3321 Aerodynamic Particle Size (APS) analyzer (TSI, 2012a) and a scanning mobility particle sizer (TSI, 2012b) (SMPS) (TSI, Shoreview, MN). The APS/SMPS measured the size-segregated particle number concentration with and without the cyclone being tested. The number concentrations for each size bin of the APS/SMPS measurements for the three AF particle size distributions were summed to determine the overall number distribution with and without the device. Using the summed number concentrations for each size bin, penetration by particle size was calculated as the particle number concentration measured with the tested device divided by the background concentration determined using the mean number concentration immediately preceding and

following the device measurement. The penetration vs. particle size graph for each device was inspected to obtain the particle size associated with the 50% ratio ( $d_{50}$ ).

**Experimental Design to Confirm Particle Separation by the MCSA:** A schematic showing the experimental design used to evaluate the ability of the MCSA to collect size-segregated crystalline silica is presented in Figure 4. These tests were performed using a Marple chamber at the Pittsburgh campus of the Office of Mine Safety and Health Research (OMSHR) (Figure 5).



**Figure 5: Marple chamber at the Office of Mine Safety and Health laboratory.**

The Marple chamber provides a uniform atmosphere of dust concentrations and maintains good control of test variables (Marple, 1983). During this evaluation the concentration of crystalline silica in the Marple chamber was maintained at 10 mg/m<sup>3</sup>. This concentration was measured using the ACGIH respirable curve convention (4.0 μm cut point at 1.7 lpm) and was used to ensure sufficient mass of collected material at each size range. The sample was drawn from the Marple chamber (Figure 4) using conductive tubing connected to the inlet of each HD cyclone, the first cyclone in the MCSA.

The ability of the MCSA to size-segregate the crystalline silica was initially confirmed, in the air, before and after each cyclone stage. Once collected, the particle size distribution of each size fraction was measured using light scattering techniques, to further confirm the size distributions. As a final confirmation, scanning electron microscopy was used to collect images of each size fraction.

**Confirmation of MCSA Design and Construction:** The MCSA was assembled as described above. After assembly, the flow rates were verified to be 2.2 lpm through the first two stages and 4.4 lpm through the second two stages. After flow rate verification the MCSA collected particles for 102 hours. The researchers were then able to successfully extract particles from each stage of the MCSA with minimal handling steps and in a form and quantity allowing for additional analysis. This data confirms the successful design and construction of the MCSA to enable collection of particles at four separate stages. The remaining paragraphs in this section, report the results of measurements aimed at demonstrating that the crystalline silica particles collected at each MCSA stage fall into four distinct size ranges.

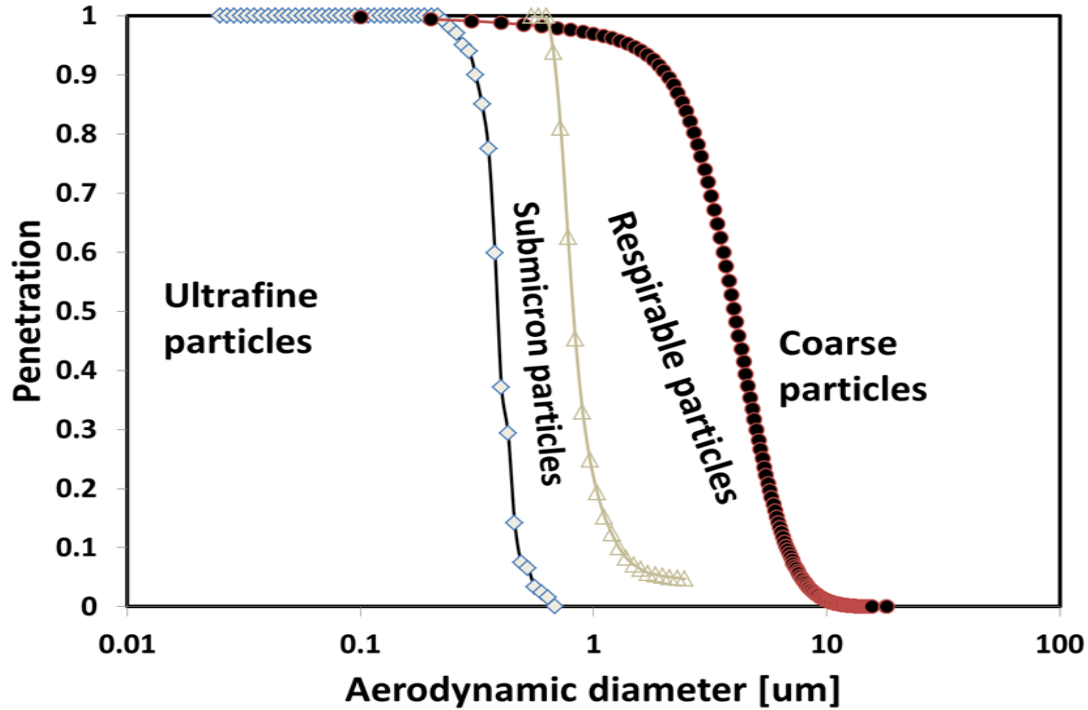
### Confirmation of Size Distribution of Airborne Particles Measured with SMPS and

**APS:** The measured specifications for cyclones used at each stage of the MCSA are presented in Table 1. Figure 6 shows the penetration curve for each stage of this sampling system as calculated using the method summarized in the methods section. These data show the SCC flowing at 2.2 lpm had a measured  $d_{50}$  of 0.74  $\mu\text{m}$  and the SCC flowing at 4.4 lpm had a much smaller  $d_{50}$  of 0.38 $\mu\text{m}$ .

**Table 1: Specifications for cyclones used in the multi-cyclone sampling array.**

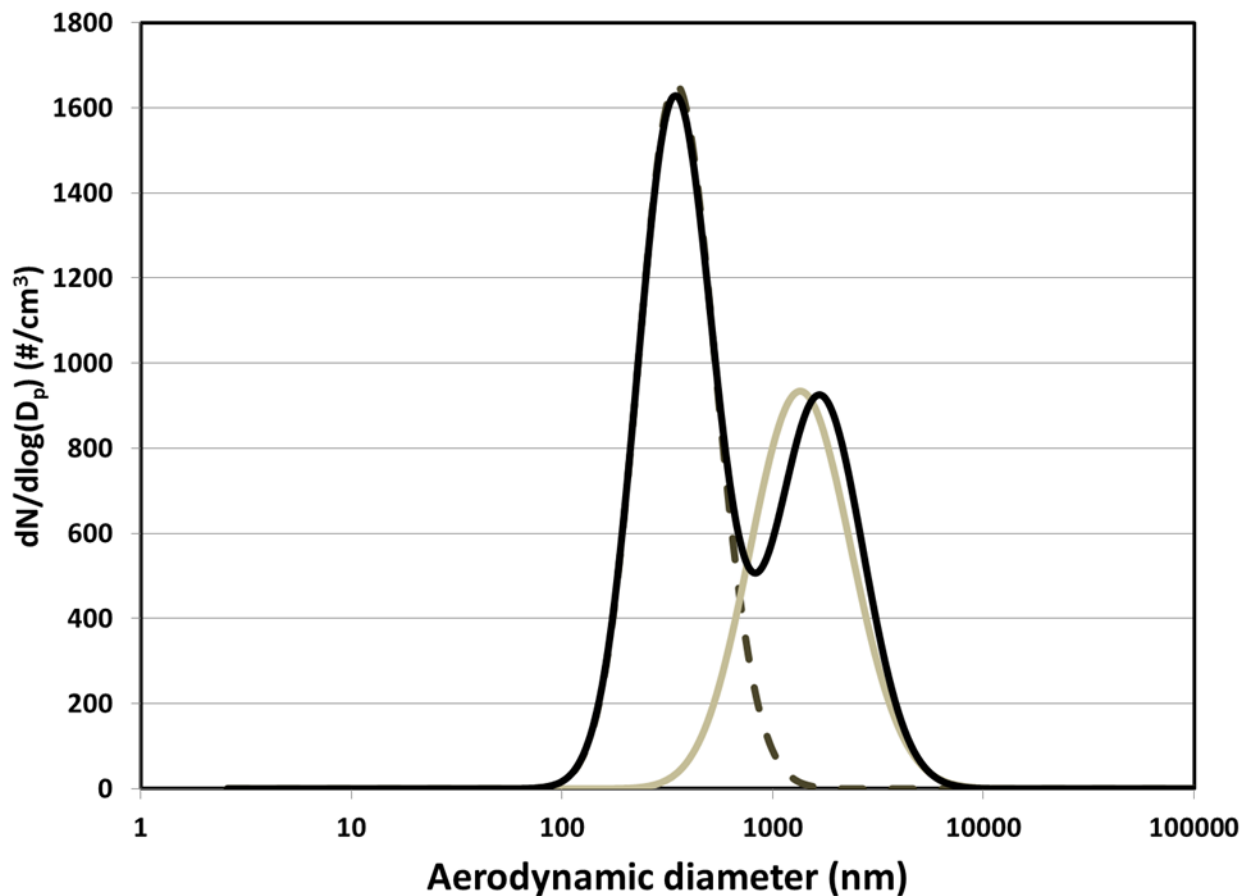
Cyclone	Flow rate (lpm)	$d_{50}$ ( $\mu\text{m}$ )
HD*	2.2	4.0
SCC 2.2	2.2	0.74
SCC 4.4	4.4	0.38

\* The information presented here for the HD cyclone comes from BGI Inc. product specifications.



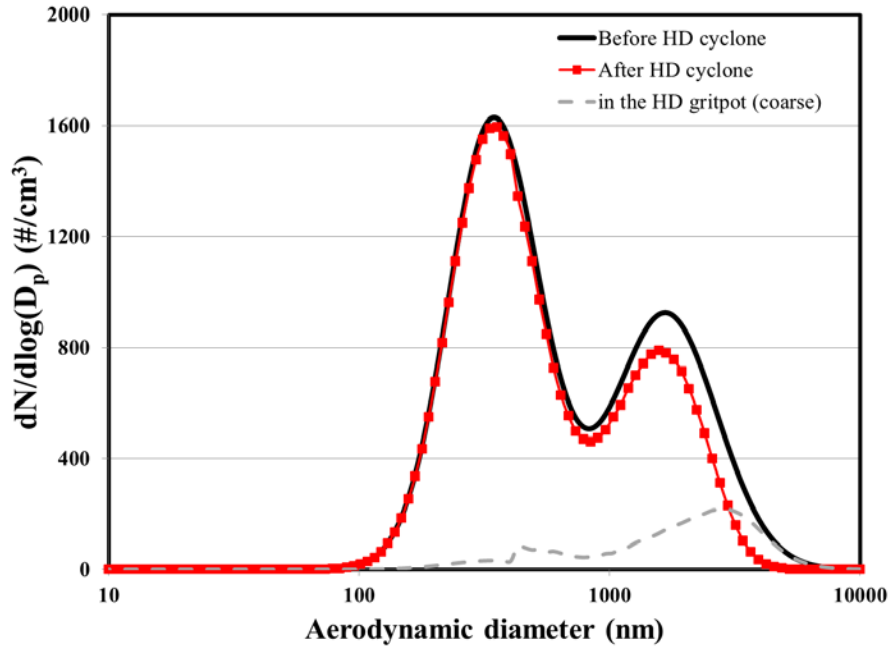
**Figure 6: Aerosol penetration curve for each sampling stage calculated using AF.**

Figure 7 presents the size distribution, on a number concentration basis, of particles for the crystalline silica base material used in this study. As discussed previously, because of the large range in particle size of the base material, this size distribution was calculated using data from both the APS and SMPS. This crystalline silica base material shows a bi-modal distribution ranging in particle size from 100 to 10,000 nanometers.



**Figure 7: Size distribution of crystalline silica base material measured in the airstream (dotted line – SMPS, tan line-APS, solid black line – merged data).**

Figure 8 presents the size distribution of the particles collected at each stage (A– C), on a number concentration basis, calculated from SMPS/APS data using the method summarized in the methods section. In addition, these figures show the particle size distributions of the airborne particles, both before and after each cyclone stage. In Figure 8C, the size distribution of particles collected on the filter includes the particles penetrating SCC 4.4.



**Figure 8A:** Size distribution of coarse particles collected by HD cyclone (dotted line). These data were calculated from SMPS/APS measurements of the airstream before (black line) and after (square markers) the HD cyclone.

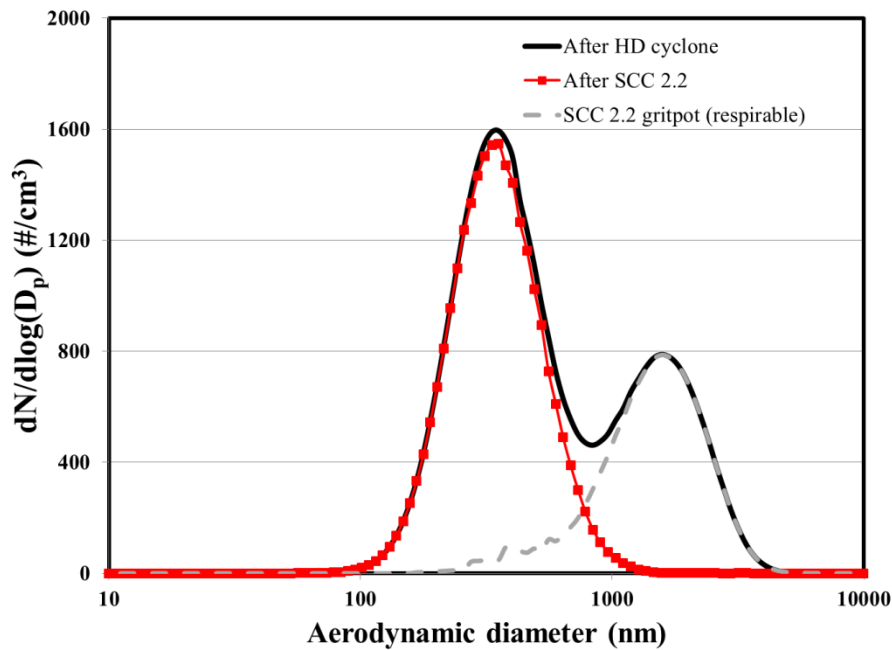


**Figure 8B:** Size distribution of respirable particles collected by SCC 2.2 cyclone (dotted line). These data were calculated from SMPS/APS measurements of the airstream after the HD cyclone (black line) and after the SCC 2.2 (square marker).

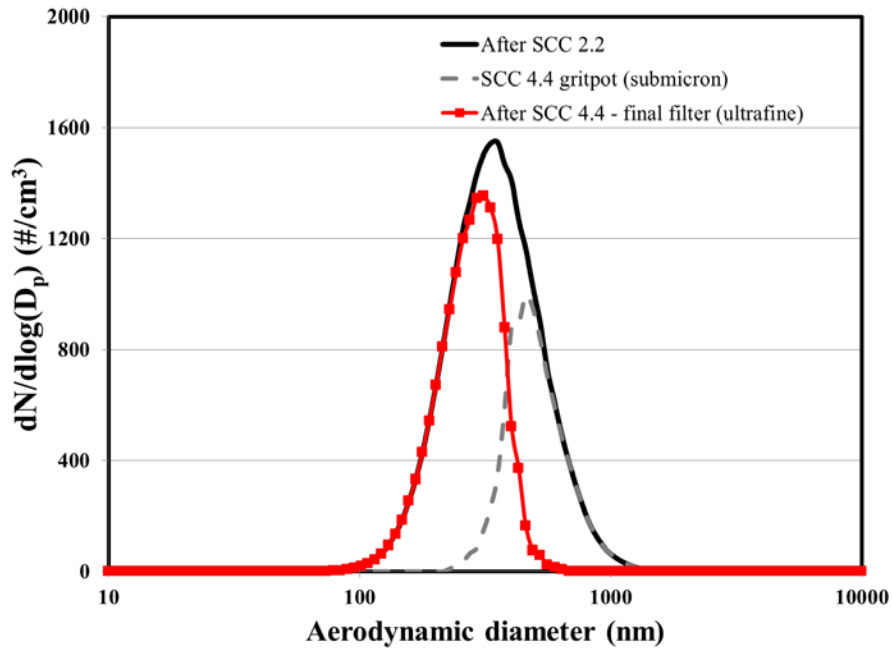


**Figure 8C: Size distribution of submicron and ultrafine particles collected by SCC 4.4 cyclone (gray-dotted line) and filter (square marker), respectively. These data were calculated from SMPS/APS measurements of the airstream after the SCC 2.2 (black line) and after the SCC 4.4 (square markers).**

**Confirmation of Size Distribution of Collected Particles Measured with DLS/LLS:**

The data in Figure 8 show the size distribution of particles collected by each cyclone and filter, calculated from air measurements. In order to confirm these air measurements, the size distribution of the particles collected at each cyclone stage and on the filter was measured using DLS/LLS. Figure 9 shows the size distributions, on an incremental volume percent basis, calculated from the light scattering data for the particles collected at each stage. Table 2 presents the geometric mean diameter and standard deviation describing the size distribution of these particles.

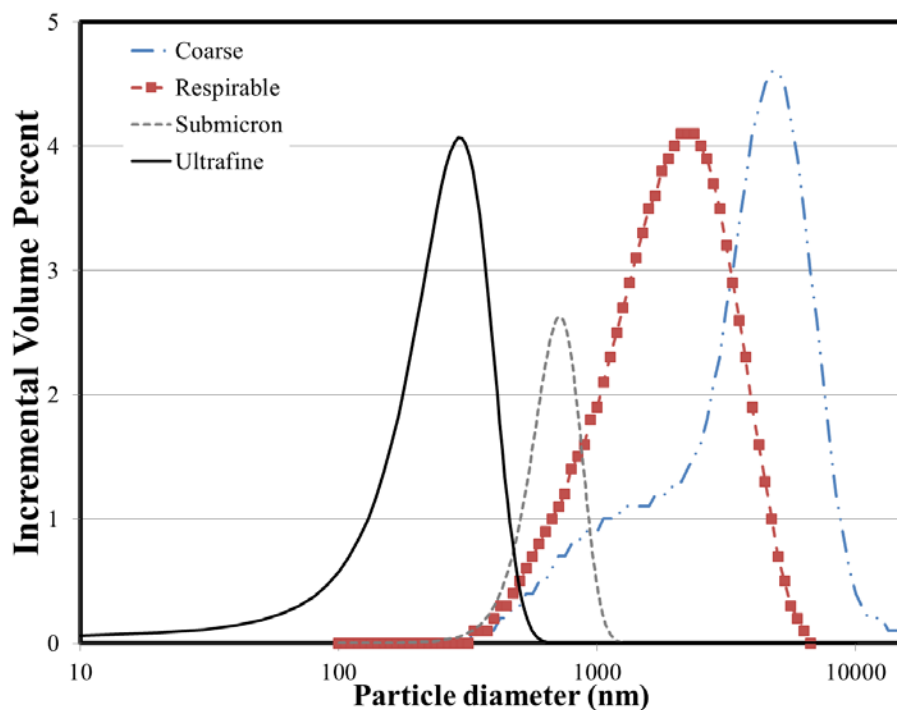


**Figure 9: Size distribution of crystalline particles from each stage of the MCSA method, calculated from light scattering data.**

**Table 2: Mean particle diameter for each size range using DLS/LLS data.**

Particle name	Mean ( $\mu\text{m}$ )	Standard deviation
Coarse	4.092	2.386
Respirable	2.123	1.146
Submicron	0.716	0.152
Ultrafine	0.294	0.098

### **Confirmation of Size Distribution of Collected Particles with Scanning Electron**

**Microscopy:** SEM images, at 5,000X magnification, of the particles collected at the different stages are presented in Figure 10 A - D. These images provide qualitative visual evidence of the different sizes of particles collected at each cyclone stage. In addition, these images confirm the crystalline structure of the silicon dioxide. The EDS analysis confirmed that the imaged particles, from each size range, were silicon dioxide (spectra not shown).

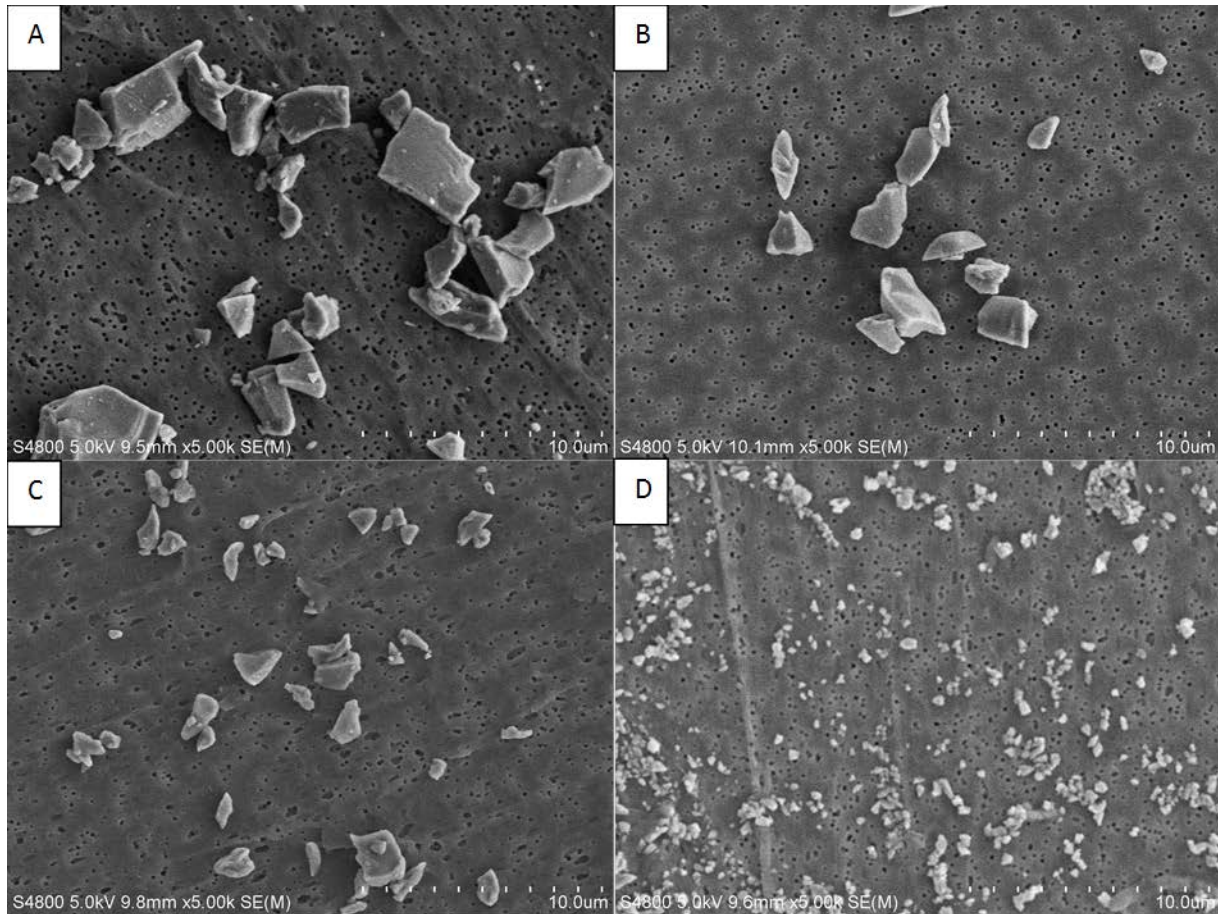


**Figure 10: SEM photographs at 5,000 magnification of crystalline silica particles retrieved from Higgins Dewell cyclone: (coarse) (A), SCC 2.2 (respirable) (B), SCC 4.4 (submicron) (C), and Filter (ultrafine) (D).**

**Note that the scale is the same for each image.**

**Mass of Particles Collected at each Stage:** The total particle mass collected at each stage during 102 hours of sampling crystalline silica in the Marple chamber at an average mass concentration of  $10 \text{ mg/m}^3$  is presented in Table 3. During this study, the average removal efficiency of the ultrafine crystalline silica particles from the filter was 90%.

**Table 3: Mass of crystalline silica particles collected at each MCSA stage.**

Particle Size	Particle mass (mg)
Coarse	351.31
Respirable	244.90
Submicron	4.60
Ultrafine	0.21

## 2.5 DISCUSSION

The results discussed above show that the MCSA can be used successfully to collect size-segregated samples at mass quantities necessary for toxicological sampling. The SMPS/APS data confirmed, through air measurements, that the MCSA can be used to achieve distinct separation according to particle size as prescribed by the design of the cyclone. In further analyzing the particle size distributions of the collected particles shown in Figure 9, the difference in the sharpness of collection efficiency between the HD cyclone and the SCC becomes readily apparent, and corroborates the measurements presented in Figure 6. The distribution of these particles is much wider than that collected from the sharp cut cyclones. This data points to the importance of using cyclones with the sharpest cutpoint possible when attempting to separate particles into distinct size ranges.

The DLS/LLS data corroborate the data presented for the APS/SMPS and show distinct size ranges for particles collected at each cyclone stage and on the filter. As with the APS/SMPS

data, the distribution for the particles in the coarse and respirable size ranges is much broader than the distribution for the submicron and ultrafine ranges.

The SEM images provide qualitative visual evidence of the different sizes of particles collected at each cyclone stage and confirmed the crystalline structure of the silicon dioxide. The EDS data confirmed that the collected particles were silicon dioxide. The ability to perform SEM/EDS analysis on the particles collected using the MCSA is critical when sampling in occupational environments due to the potential for particles of different sizes to have distinct elemental fingerprints. This is especially important in an industry such as mining which is working toward eliminating silicosis among mine workers. The possibility that silica is present in a greater percentage in smaller particles can be confirmed using this type of analysis.

The mass data shows that this method allows for the recovery of measurable mass in all particle sizes, particularly the ultrafine. As expected, the highest percentage of particle mass was collected in the coarse particle size and the lowest percentage of particle mass was measured in the ultrafine particle size. The significance of this data is that this method enables the collection of a sufficient quantity of particles at each method stage to be used in toxicity testing or physical/chemical characterization.

Several research groups have published data on systems used to collect size-segregated samples for toxicological sampling (Ramgolam et al., 2009, Stephanie et al., 2011, Ruusunen et al., 2011, Kim et al., 2001a, Sillanpaa et al., 2003, Steenhof et al., 2011). In each system described in this research, impactors were used to achieve separation between particle sizes. The impaction method is used as a means of size selection for ambient and occupational air sampling because it provides sharp size-selective sampling. Since the 1960's, cascade impactors, instruments in which the aerosol flows through successive impactor stages, have been used

extensively to measure the size distribution of ambient aerosols on a mass basis (Hinds, 1999). However, when attempting to sample particles at masses necessary for toxicological tests, overloading of the impactors can occur (Stephanie et al., 2011). Overloading is a process where layers of previously collected particles result in a change of particle size collected at each stage, through particle bounce or de-agglomeration (Vanderpool et al., 2001). Overloading of impactors is a concern due to the potential of changing the representative size distribution, of each stage, over the entire sampling period (Volkwein, 2004, Virtanen et al., 2010). Because substrate overloading results in larger particles being collected on substrates for smaller particles, and given the relative masses between large and small particles, the unintended intrusion of large particles on small particle substrates could result in a positive bias towards mass of small particles (Kenny et al., 2000). In addition, when these overloaded substrates are then used for toxicological tests, the cells may be exposed to particles that are larger than intended.

Cyclones have also been widely used for size-selective particle sampling. Typically, cyclones can be designed for applications needing a specific  $d_{50}$  and sharpness of separation, using the cyclone's body dimensions and flow rate through the cyclone (Kenny and Gussman, 1997). Cyclones offer a suitable alternative to impactors if they supply a similar size cut point, sharpness and mass penetration (Kenny et al., 2000). Kenny et al. (Kenny et al., 2000) showed that the SCC provides a sufficiently sharp cut for ambient monitoring applications. In addition, their research showed that impactors loaded with < 3 mg of dust resulted in deterioration in the impactors' performance. In the present evaluation, the mass of particle loading, in over 100 hours of sampling, significantly exceeded the mass loading that Kenny reported as having resulted in deteriorated performance by the impactors.

The loading effects noted for the impactor precludes its use for collection of a large mass of size-segregated particles. However, cyclonic devices, such as those used in this study, were demonstrated to have significant advantages over impactors for extended operation and high mass loadings (Kenny et al., 2004). In this study the MCSA successfully segregated mass loadings exceeding 600 mg with no detectable deterioration of the cyclone cutpoint performance.

## 2.6 CONCLUSION

This study focused on the development and laboratory evaluation of a multi-cyclone sampling array, capable of separating occupational aerosols into distinct size ranges, over extended sampling periods to allow for collection of sufficient quantity of particles for toxicological testing and physical/chemical characterization.

Several limitations arise when attempting to collect sufficient mass of ultrafine particles from an occupational or ambient environment, including; (1) the potential for a high mass concentration of the aerosol mixture, (2) the probability that the bigger particles will make-up a large percentage of the overall aerosol mass concentration, and the necessity of separating these particles while avoiding their inclusion in the smaller particle collection bins, and (3) the need for a compact and simple system that can be used in challenging occupational environments.

The MCSA was designed with these limitations in mind. The results presented here, using SMPS, APS, DLS/LLS and SEM/EDS data, show that this multi-cyclone system was able to successfully collect distinct size-segregated particles at appropriate masses to perform toxicological sampling.

The crystalline silica used in this testing ranged in size from  $>10\mu\text{m}$  to  $<0.1\ \mu\text{m}$ . The scientific literature, reporting on crystalline silica toxicology, uses material with a large size range of the particles without regard to the potentially distinct effects of the different particle sizes. To our knowledge this is the first method that has been shown to successfully separate airborne crystalline silica into distinct size groups. As discussed in the Introduction, these ultrafine crystalline silica particles are potentially underrepresented by the occupational mass standards, and this research is the initial step in evaluating whether these mass standards need adjusting. In addition, if the ultrafine particles prove to be more biologically active, then control technologies currently used may need to be re-evaluated and adjusted to more successfully control exposure to these smaller particles.

Although this research focused on crystalline silica, this sampling method can be used for size-segregated sampling of a wide variety of occupational or environmental aerosols. Because this method allows for the concurrent collection of four different sizes of aerosols, it enables scientists to conduct physical and chemical evaluations, as well as *in vivo* or *in vitro* evaluations, of these simultaneously collected aerosols.

**3.0 DIFFERENTIAL ACTIVATION OF MURINE ALVEOLAR  
MACROPHAGES BY SIZE-SEGREGATED CRYSTALLINE SILICA**

Steven E. Mischler<sup>1</sup>, Emanuele G. Cauda<sup>1</sup>, Michelangelo Di Giuseppe<sup>2</sup>, Linda J. McWilliams<sup>1</sup>,  
Claudette St. Croix<sup>3</sup>, Ming Sun<sup>4</sup>, Jonathan Franks<sup>4</sup>, Luis A. Ortiz<sup>2</sup>

<sup>1</sup> National Institute for Occupational Safety and Health, Office of Mine Safety and Health  
Research, Pittsburgh, Pennsylvania

<sup>2</sup> University of Pittsburgh, Department of Environmental and Occupational Health, Pittsburgh,  
Pennsylvania

<sup>3</sup> University of Pittsburgh, Center for Biological Imaging, Environmental and Occupational  
Health,

<sup>4</sup> University of Pittsburgh, Center for Biological Imaging

**Adapted from publication submitted to the Journal, Inhalation Toxicology**

### 3.1 ABSTRACT

Occupational exposure to crystalline silica is a well-established occupational hazard. Once in the lung, crystalline silica particles can result in the activation of alveolar macrophages potentially leading to silicosis, a fibrotic lung disease. Because the activation of alveolar macrophages is the beginning step in a complicated inflammatory cascade, it is necessary to define the particle characteristics resulting in this activation. The aim of this research was to determine the effect of the size of crystalline silica particles on the activation of macrophages. RAW 264.7 macrophages were exposed to four different sizes of crystalline silica and their activation was measured using electron microscopy, reactive oxygen species (ROS) generation by mitochondria, and cytokine expression. These data identified differences in particle uptake and formation of subcellular organelles based on particle size. In addition, these data show that the smallest particles, with a geometric mean of 0.3  $\mu\text{m}$ , significantly increase the generation of mitochondrial ROS and the expression of cytokines when compared to larger crystalline silica particles, with a geometric mean of 4.1  $\mu\text{m}$ .

## 3.2 INTRODUCTION

Occupational exposure to crystalline silica (CS) affects at least 1.7 million US workers (NIOSH, 2002) and is associated with the development of silicosis, a fibrotic lung disease which is one of the most important occupational diseases worldwide (Greenberg et al., 2007, WHO, 2007, Leung et al., 2012). The National Institute for Occupational Safety and Health (NIOSH) reported that 300 silicosis-related deaths occurred each year in the United States between 1991 and 1995 (NIOSH, 2013). During those same years China recorded 24,000 silicosis-related deaths per year (WHO, 2000). These numbers indicate that silicosis remains a fundamental occupational exposure problem in both the developing and developed countries (Huaux, 2007).

Exposure to CS occurs in many occupations and industries. The United States Occupational Safety and Health Administration (OSHA) measured detectable levels of respirable CS in samples collected in 255 different industries (NIOSH, 2002). In general, silica exposure will occur in any occupation which includes grinding or mechanically breaking material containing silica (mining, construction) or handling fine particles containing silica, such as silica sand (fracking) (Sirianni et al., 2008, Leung et al., 2012, Beaudry et al., 2013, Hall et al., 2013, McKinney et al., 2013, Sauve et al., 2013).

Although occupational exposure to CS and the related health effects have been well documented in the scientific literature, many uncertainties still exist including the effect of the crystals surface characteristics, including particle size, on the development of disease (Wiessner et al., 1989, Fubini and Hubbard, 2003, Bodo et al., 2007, Kajiwara et al., 2007, Wang et al., 2007, Sirianni et al., 2008, Leclerc et al., 2012). Most atmospheric studies suggest that the concentration of smaller particles correlate better with adverse health effects than the

concentration of larger particles (Churg and Brauer, 2000, Donaldson and MacNee, 2001, Kajiwara et al., 2007, Knol et al., 2009, Pope et al., 2009); however, there is little size dependent toxicity data concerning CS. One difficulty in completing size-dependent toxicity studies with CS is the difficulty in separating the occupational aerosol into distinct size ranges and in necessary quantities for toxicological studies. Recently our group published research on a novel multi-cyclone sampling array which enables the separation of occupational aerosols into distinct size ranges and in quantities needed for toxicological research (Mischler et al., 2013).

Because smaller particles have a higher surface area per unit mass when compared to larger particles, smaller particles may more readily start potential negative biological reactions, such as inflammation (Monteiller et al., 2007). Chronic inflammation has been implicated in the pathogenesis of silicosis. In this scenario, the immune cells (alveolar macrophages, epithelial cells and fibroblasts) are activated and release a host of inflammatory cytokines and generate reactive oxygen species (ROS) resulting in the recruitment of additional inflammatory cells, predominantly alveolar macrophages. The influx of additional inflammatory cells and release of ROS damages pulmonary architecture causing accumulation of connective tissue products (Mossman and Churg, 1998, Fubini and Hubbard, 2003, Rimal et al., 2005, Huaux, 2007, Hamilton et al., 2008). Knowledge of the degree to which particle size affects the activation of macrophages and the resulting ROS generation and inflammatory response is necessary for fully elucidating the mechanisms leading to silicosis from occupational exposure to crystalline silica.

In the present *in vitro* study the macrophage response to different-sized crystalline silica particles was evaluated using the mouse monocyte-macrophage RAW 264.7 cell line. Airborne CS particles were separated into four distinct size ranges using the multi-cyclone sampling array. The RAW 264.7 macrophages (AM) were exposed to four different sizes of CS and their

activation was measured using electron microscopy, mitochondrial ROS (mROS) generation and cytokine expression.

### 3.3 METHODS

**Particles used for method evaluation:** The crystalline silica (SiO<sub>2</sub> quartz, 99.9%, 1 $\mu$ m, Stock #: 4807YL) used in this study was purchased from Nanostructured & Amorphous Materials, Inc. (Houston, TX). Before particles were used in the experiment they were baked at 220°C for 24 hours to destroy potential contaminating endotoxins.

**Silica particle suspension and characterization:** Stock silica suspensions were prepared by adding serum free DMEM into a measured mass of crystalline silica particles to achieve the desired particle concentrations. For cytokine analysis an exposure concentration of 50  $\mu$ g/cm<sup>2</sup> was used for all particle sizes, for live-cell experiments and Transmission electron microscopy (TEM) analysis an exposure concentration of 16.6  $\mu$ g/cm<sup>2</sup> was used for all particle sizes. The silica suspensions were used within two hours of mixing with serum-free DMEM. Before each exposure the stock solutions were sonicated for 15 minutes to ensure adequate distribution of the particles and reduce any agglomeration. After exposure the stock solutions were analyzed with dynamic light scattering to verify particle size distribution, as described previously (Mischler et al., 2013).

**Cell cultures:** Cells from the mouse monocyte-macrophage RAW 264.7 cell line were purchased from American Type Tissue Culture Collection (ATCC, Rockville, MD) and

maintained according to ATCC protocols at 37°C in a 5% CO<sub>2</sub>/95% air humidified incubator. Cells were cultured in DMEM with 10% fetal bovine serum (FBS) and penicillin-streptomycin, on 75 cm<sup>2</sup> plates. Approximately 24 hours prior to exposure the cells were plated into 6- or 12-well plates. Exposure experiments were completed when the cells were at 80% confluency.

**TEM analysis:** At one, two and four hours after exposure, cells were fixed in 2.5% glutaraldehyde in PBS and postfixed in 1% osmium tetroxide in PBS, dehydrated through a graded series of alcohols and embedded in Epon (Energy Beam Sciences, Agawam, MA). Thin (70-nm) sections were cut using a Reichert Ultracut S (Leica, Deerborn, MI), mounted on 200 mesh copper grids and counter-stained with 2% aqueous uranyl acetate for seven minutes and 1% aqueous lead citrate for two minutes. Observation was with a JEOL 1011 transmission electron microscope (Peabody, MA). After TEM images were collected, they were formatted using Adobe Photoshop for brightness and contrast. In addition, during slide preparation, if a particle was greater than 70 nm it may create stretching in the epon resin during the slicing sequence, and if stretching were severe the particle may fall out of the resin. During TEM imaging, any areas where the particles fell out will show as bright white, causing difficulty in image focusing. These images were corrected by re-coloring the white areas back to the color of the silica particles. The result may be a slight increase in the particle size for the areas that were recolored.

**Live-cell microscopy for measurement of mitochondrial ROS:** The effect of particle size on the production of mitochondrial ROS in RAW 264.7 AM was evaluated using live-cell microscopy. Mitochondrial ROS generation (as superoxide) can be measured using MitoSOX™

Red (Invitrogen, Eugene, OR), which is hydroethidine (HE) modified with a hexyl linker to a triphenylphosphonium. MitoSOX™ preferentially accumulates in the mitochondria and becomes fluorescent upon oxidation (Robinson et al., 2008). Cells were seeded on 35mm glass bottom dishes (MatTek Corporation, Ashland, MA) and incubated with 5 μM of MitoSOX™ Red for 15 minutes at 37 °C. Cells were washed with Phosphate-Buffered Saline (PBS), the media replaced with exposure media and the dish inserted into a closed, thermo-controlled (37°C) stage top incubator (Tokai Hit Co., Shizuoka-ken, Japan) atop the motorized stage of an inverted Nikon TiE fluorescent microscope (Nikon Inc., Melville, NY) equipped with a 60X oil immersion optic (Nikon, CFI PlanFluor, NA 1.43) and NIS Elements Software. MitoSOX™ Red was excited using a Lumencor diode-pumped light engine (SpectraX, Lumencor Inc., Beaverton OR) and detected using a DsRed longpass filter set (Chroma Technology Corp) and ORCA-Flash4.0 sCMOS camera (HAMAMATSU Corporation, Bridgewater, NJ). Data was collected on approximately 80 to 100 cells per stage position, with eight to ten stage positions in each of the separate experiments for 180 minutes. Data were analyzed using NIS Elements (Nikon Inc., Melville, NY). Data from three independent analyses for each particle size were used in the statistical calculations. Stage positions in which the particles did not result in AM generation of ROS were not used in the statistical analysis.

**Cytokine analysis:** The effect of particle size on expression of inflammatory cytokines was evaluated using the Bio-Plex multiplex magnetic bead technology (LMC0001, Mouse Cytokine 20-Plex, Invitrogen/Life Technologies, Carlsbad, CA). This assay simultaneously measured the concentration of 20 cytokines in the cellular supernatant. At least three independent experiments were conducted for cytokine expression. Each experiment was conducted using a

nested triplicate model where each exposure was run in triplicate and each sample was analyzed in triplicate. For every experiment both a positive and negative control were used. For the negative controls the cells were treated only with serum free DMEM medium. For the positive control, the cells were treated with serum free DMEM, containing 200 ng/ml of LPS. In each experiment cells were exposed to one of four different particle stock solutions, described above, for two, four or eight hours prior to collection of the supernatant. After collection, supernatant was stored at -80°C until analysis.

**Statistical Analysis of mitochondrial ROS measurements:** To help understand how particle size affects the production of reactive oxygen species in the mitochondria (mROS) in AM we exposed AM to both UF and C particles over a 3-hour exposure period and measured mROS production using the superoxide indicator MitoSOX™ Red to measure increase in fluorescence.

In this study, fluorescence was measured at approximately three-minute intervals over a period of 193 minutes in samples exposed to UF and C particles. Measurements were taken on three samples exposed to each of the two particle sizes at each of the 65 time points. For the purpose of data analysis, the 65 time points were grouped into 30-minute periods, resulting in a larger sample size for each statistical test, and therefore greater statistical power. Data were analyzed by six independent-samples t-tests comparing mean fluorescence values across the two conditions for each time period. A p-value less than 0.05 was considered to be statistically significant.

Because examination of distributions of fluorescence values showed a departure from normality, data were also analyzed using the Wilcoxin test, which is the non-parametric

counterpart of the t-test. However, since results of the Wilcoxin test agreed with the results of the t-test in every case, only results of the t-tests will be reported.

**Statistical analysis for cytokine expression:** Data are presented as mean and standard deviation. Nonparametric statistical tests, which make no assumption about the distribution of the data, were used to investigate differences of cytokine expression from exposure to the different particle sizes. A p-value less than or equal to 0.10 was considered to be statistically significant. The Kruskal-Wallis test is the nonparametric alternative to the one-way analysis of variance (ANOVA). This test was used to compare mean ranks among all the samples. If the results of this test were statistically significant the null hypothesis of no difference was rejected and post-hoc tests were run to search for pair-wise differences. For the latter analysis, the Wilcoxon rank sum test, the nonparametric analogue to the t-test for independent samples was used. For both the Kruskal-Wallis and Wilcoxon tests, exact probabilities were calculated (Rosner, 1990).

### 3.4 RESULTS

**Particle extraction from MCSA:** The size-segregated particles were collected from the grit pot of each cyclone using the following procedure. The grit pot was first inverted and tapped on the outside, allowing the particles to fall out of the grit pot and be collected onto an aluminum collection disk. Any particles which did not fall from the grit pot or particles which remained in the cone were scrapped from these surfaces using a plastic or wooden scrapping tool. Complete recovery of the particles from each cyclone was not important, only that the particles could be collected in sufficient mass, at each stage, for further characterization and analysis. Once the particles were fully recovered from each cyclone the particles were weighed and stored for later characterization and testing.

The pre-weighed filter, containing the smallest size range of particles, was post-weighed to determine the mass of particles collected on the filter. The particles collected on the filter were then removed using the following procedure; 1) The filter containing the particles was placed in a 15 ml centrifugal test tube, submerged in 5 ml of ultrapure deionized water and sonicated for five minutes, 2) after sonication, the filter was removed from the first tube and placed in a second tube. Five ml of ultrapure deionized water was added to the second tube, the filter was submerged in the water and sonicated for five minutes, 3) after sonication, the water was poured into the first tube, which now contains 10 ml of particle laden water, 4) another 5 ml of ultrapure deionized water was then added to the tube containing the filter, the filter was submerged into the water and sonicated for five minutes, 5) after sonication, the 5 ml of water was poured into the first tube, which now contains 15 ml of particle laden water, 6) the tube containing the 15 ml

of particle laden water was then centrifuged for seven minutes at 3901 relative centrifugal force (RCF), 7) after centrifugation, the supernatant was removed leaving the particles at the bottom of the tube, 8) serum-free Dulbecco's Modified Eagle's Medium (DMEM) was then added to the tube containing the particles to achieve the desired exposure concentration. The necessary volume of DMEM added was calculated based on the post-weight of the filter, 9) once the particles were removed from the filter, the filter was dried and reweighed to verify the mass of particles removed. During this study, the average removal efficiency of the ultrafine CS particles from the filter was 90% as reported previously (Mischler et al., 2013).

**Confirmation of Size Distribution of particles used in exposure:** The mean and standard deviation of the particles in each size range is presented in Table 4 and SEM photographs at 5,000X magnification of each size range are presented in Figure 11.

**Table 4: Mean particle diameter and standard deviation for each size range using DLS/LLS data.**

Particle name	Mean ( $\mu\text{m}$ )	Standard deviation
Coarse (C)	4.092	2.386
Respirable (R)	2.123	1.146
Submicron (S)	0.716	0.152
Ultrafine (UF)	0.294	0.098

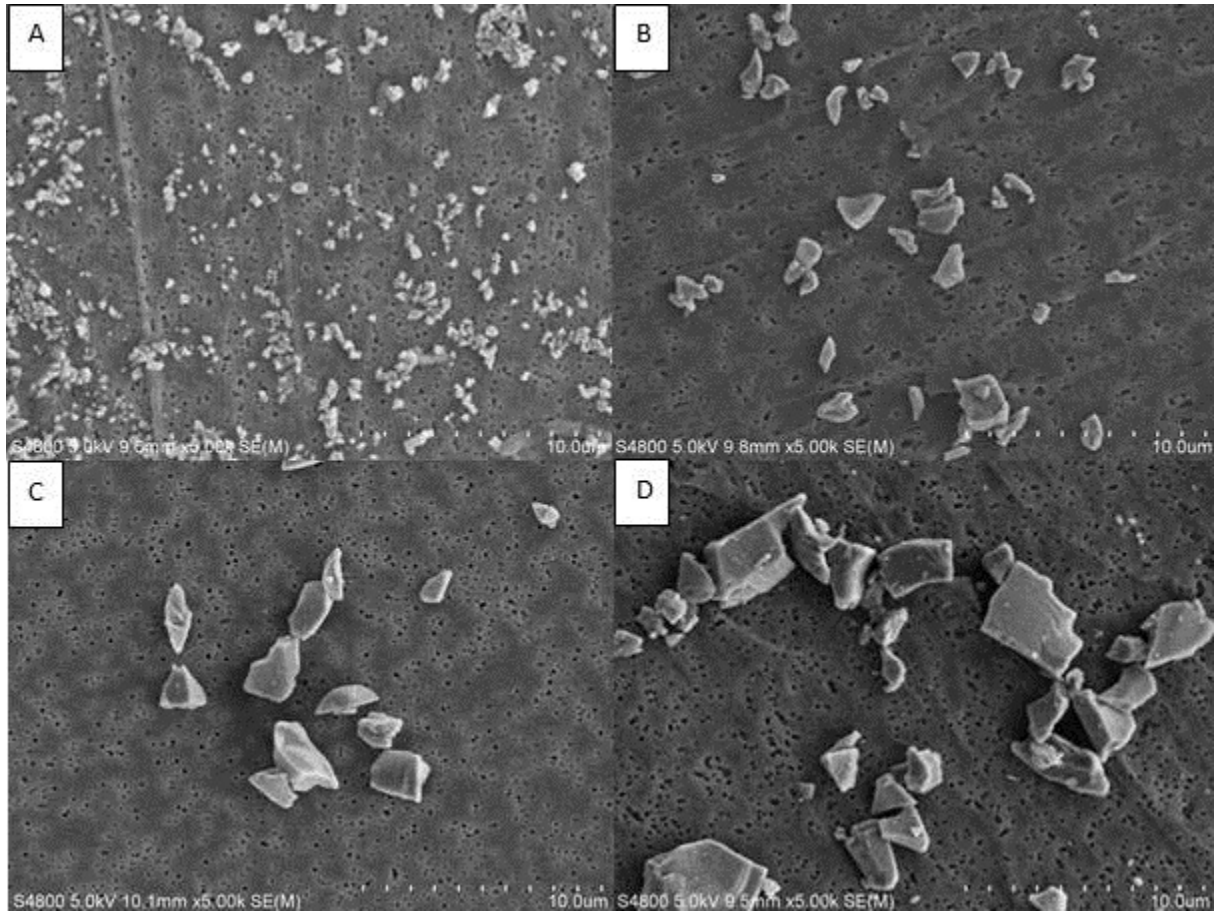
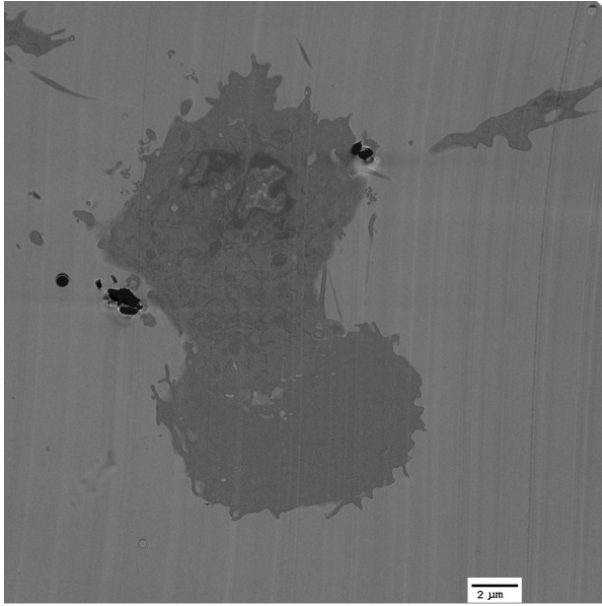


**Figure 11: SEM photographs at 5,000 magnification of crystalline silica particles used for this study: A) Ultrafine (UF), B) Submicron (S), C) Respirable (R), and D) Coarse (C).**

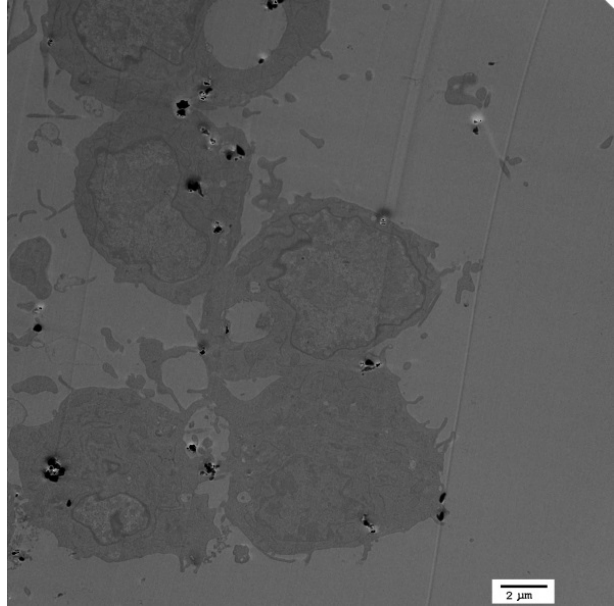
**Note that the scale is the same for each image.**

**TEM Images of RAW cells after exposure with two sizes of crystalline silica:** In order to visualize the difference in the handling of UF particles and C particles by AM, RAW 264.7 AM were exposed to UF and C particles for one, two, and four hours. At the appointed time the particles were fixed and stored until image collection, as discussed in the methods section.

Figure 12 A and B present images (6,000X magnification) of the AM cells after exposure for one hour to C and UF particles, respectively. At this time point, the images show that the UF particles are internalized more quickly and in larger numbers than the coarse particles. This result is consistent with the literature showing faster uptake of UF particles by AM. In addition, Figure 12B shows phagolysosome (PL) swelling is starting to occur in response to the UF particles. Figure 13 is a higher magnification image of an AM exposed to UF particles for one hour. In this micrograph, the silica particles are marked S, the mitochondria are marked M and W denotes a white area resulting from particles falling out of the resin, as discussed in the methods section. In Figure 3 there is no evidence of UF particles in the cytoplasm or mitochondria.

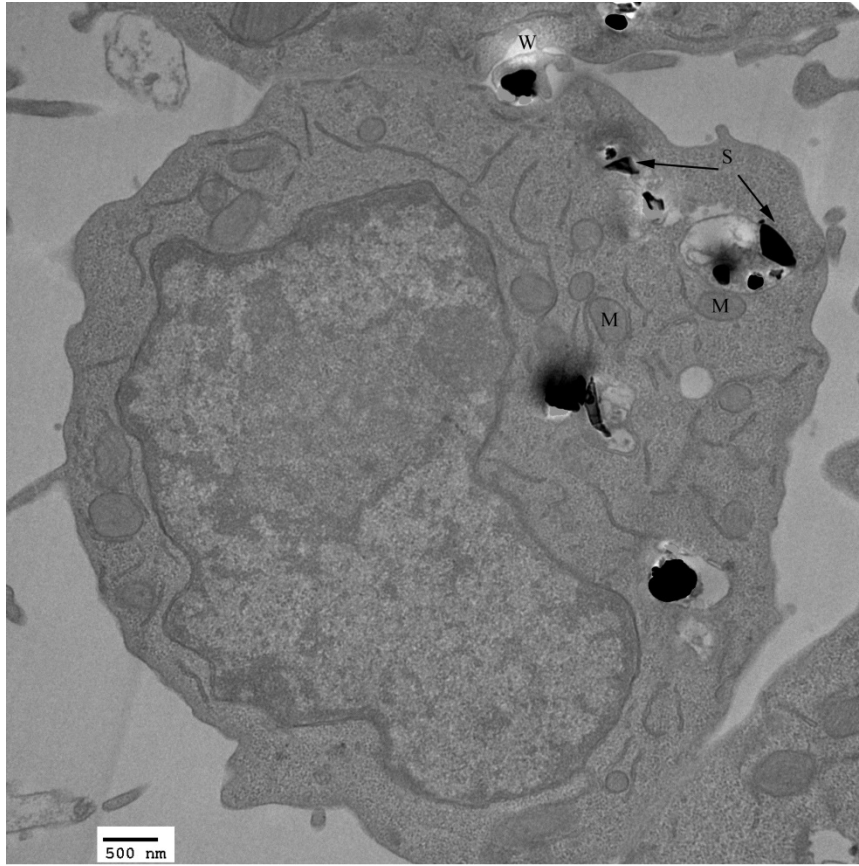


A) Coarse particles (6000X)



B) UF particles (6000X)

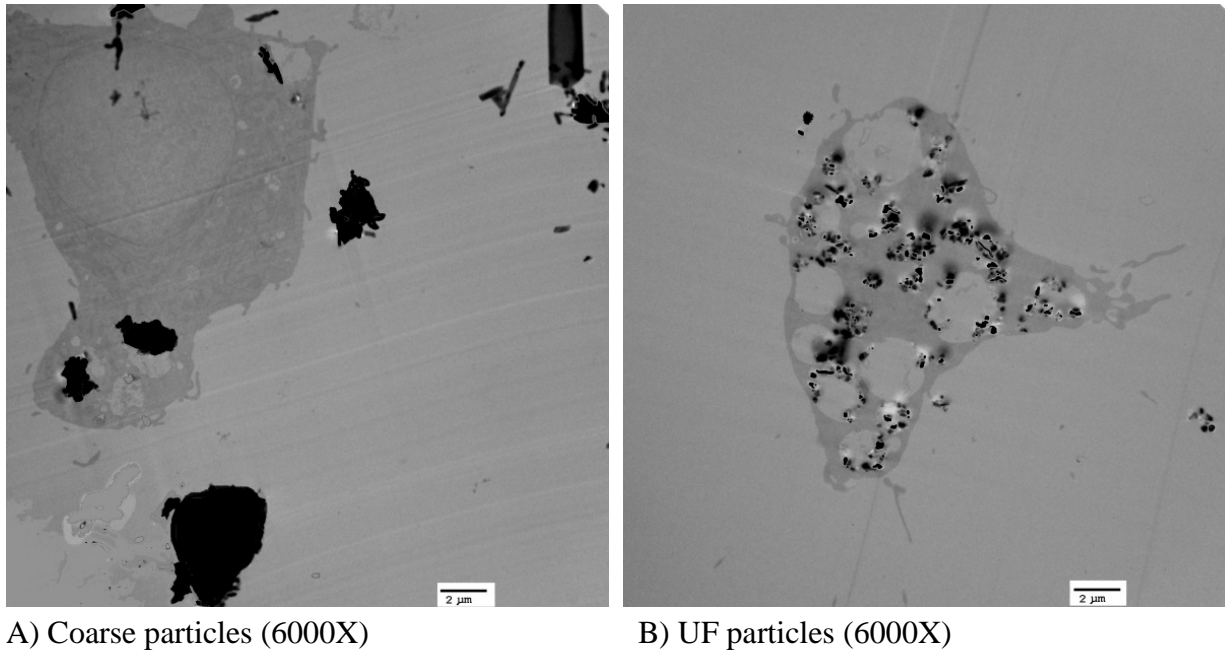
**Figure 12: TEM images after 1-hour exposure of AM to Coarse and UF particles.**



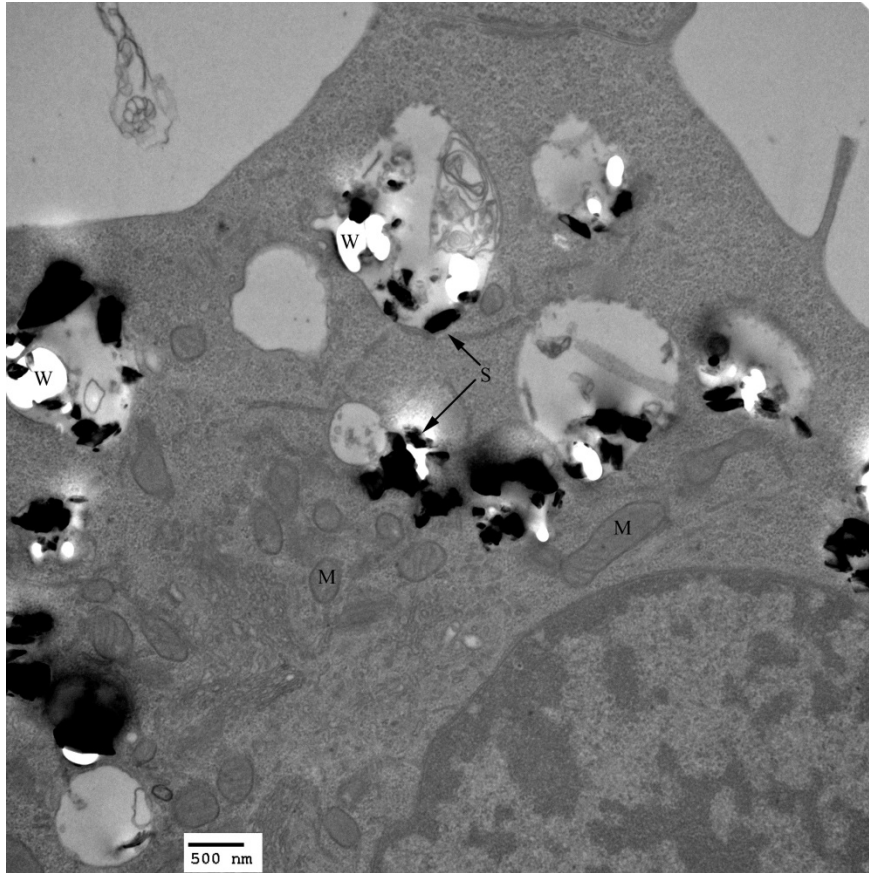
**Figure 13: High Magnification (20,000X) TEM image at AM exposed to UF particles for 1 hour.**

Figure 14 A and B present images (6,000X magnification) of the AM cells after exposure for two hours to C and UF particles, respectively. These micrographs also show that a larger number of UF particles have been internalized by this time point than the C particles, once again consistent with the literature. Figure 14A shows that by the two hour time period the C particles have been phagocytized by the AM and PL swelling is apparent. Figure 14B shows a cell with up to ten large PLs each containing numerous CS particles. In this figure the PLs are clearly swollen indicating acidification and enzyme and protease production and delivery. For the C particles, each AM is seen to have phagocytized between one and three particles; whereas, as many as 100 UF particles have been phagocytized by this time point. Figure 15 is a higher magnification

image of an AM exposed to UF particles for two hours and shows that each PL contains numerous particles as well as additional dense cellular material. In Figure 15, there is no evidence of UF particles in the cytoplasm or mitochondria.

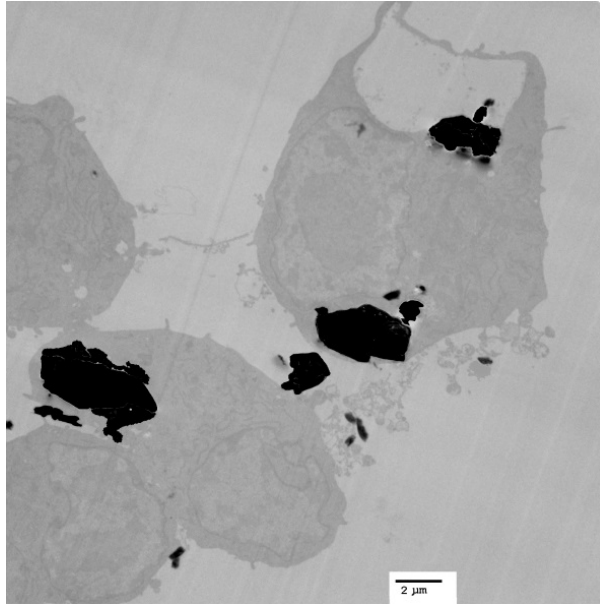


**Figure 14: TEM images after 2-hour exposure of AM to Coarse and UF particles.**

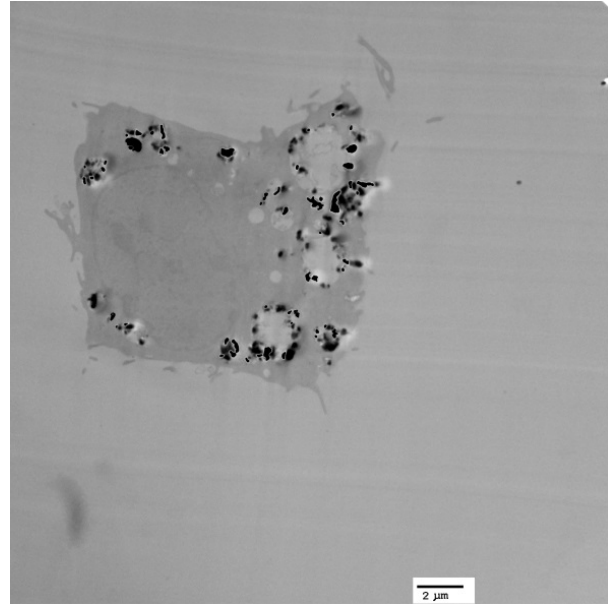


**Figure 15: High Magnification (20,000X) TEM image of AM exposed to UF particles for 2 hours.**

Figure 16 A and B present images (6,000X magnification) of the AM cells after exposure for four hours to C and UF particles, respectively. These images are similar to two hour images, where the UF particles have been phagocytized in greater number, resulting in creation of a higher number of PLs. The PLs are swollen but the membrane appears to still be intact. This can be seen more clearly in Figure 17, a higher magnification image of an AM exposed to UF particles for four hours. As noted for Figure 17 there is no evidence of UF particles in the cytoplasm or mitochondria; however, it appears that the amount of dense cellular material in each PL is greater than seen in the earlier time points.



**A) Coarse particles (6000X)**



**B) UF particles (6000X)**

**Figure 16: TEM images after 4-hour exposure of AM to Coarse and UF particles.**

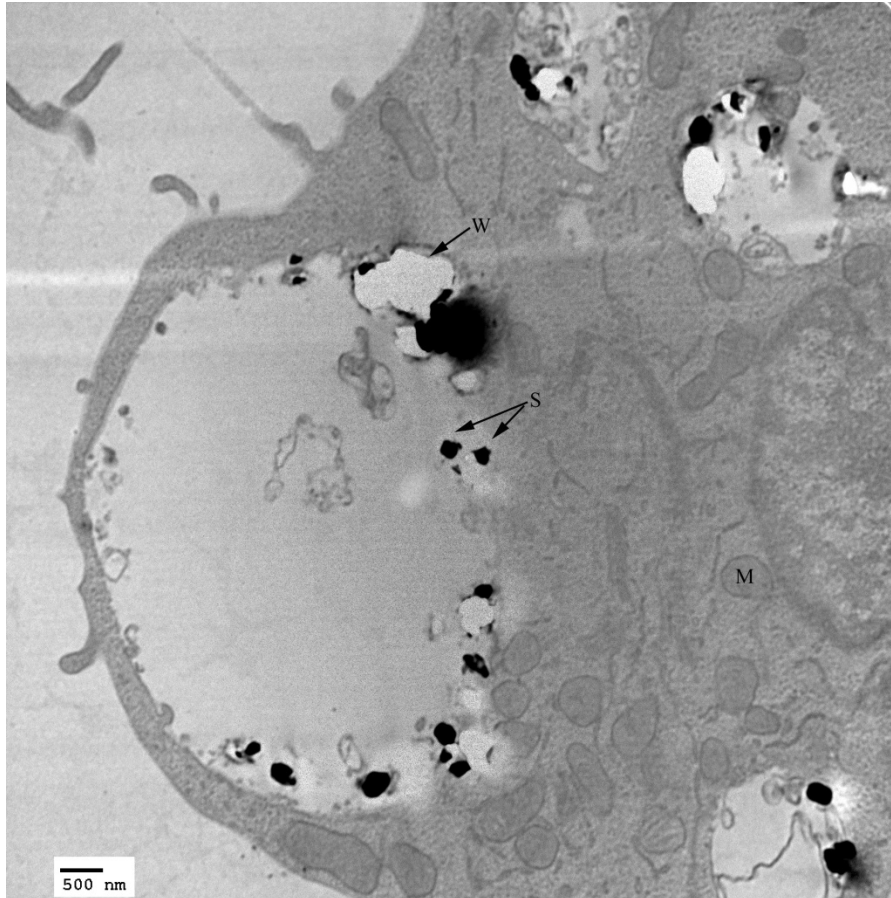


**Figure 17: High Magnification (15,000X) TEM image of AM exposed to UF particles for 4 hours.**

**Generation of Mitochondrial ROS:** To help understand how particle size affects AM activation the production of mROS in AM in response to exposure to C and UF particles was measured over a three hour period. As discussed in the methods section, for the purpose of data analysis, the 65 time points were grouped into 30-minute periods as shown in Table 5. This grouping resulted in a larger sample size for each statistical test, and therefore greater statistical power. Data from Period 7 were not analyzed because of the difference in sample size. A p-value less than 0.05 was considered to be statistically significant.

**Table 5: Grouping of Time Points for mROS statistical analysis.**

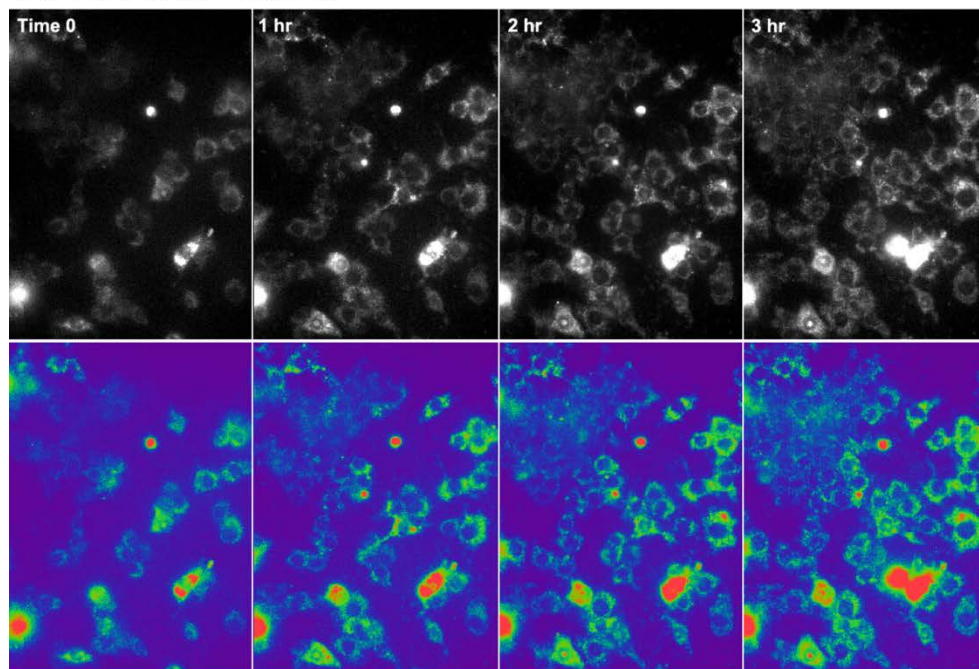
<b>Period</b>	<b>Time points (minutes)</b>	<b>Number of Time Points</b>	<b>Number of Data Points per Condition</b>
1	1, 4, 7, 10, 13, 16, 19, 22, 25, 28, 31	11	33
2	34, 37, 40, 43, 46, 49, 52, 55, 58, 61	10	30
3	64, 67, 70, 73, 76, 79, 82, 85, 88, 91	10	30
4	94, 97, 100, 103, 106, 109, 112, 115, 118, 121	10	30
5	124, 127, 130, 133, 136, 139, 142, 145, 148, 151	10	30
6	154, 157, 160, 163, 166, 169, 172, 175, 178, 181	10	30
7	184, 187, 190, 193	4	12

Means and standard deviations of fluorescence, t-values, and p-values are shown in Table 6. The assumption of equality of variances was not met for several of the tests, and in those cases p-values associated with the Satterthwaite approximation of degrees of freedom are reported. Figure 18a is a representative image from the live cell experiments taken at 0, 1, 2 and 3 hours after particle exposure and Figure 18b is a graph of the means shown in Table 6.

**Table 6: Results of Independent Samples t-tests for mROS measurements.**

<b>30</b>	Ultrafine	42.55	60.84	3.12	.004*
	Coarse	8.98	11.35		
<b>60</b>	Ultrafine	203.81	87.86	8.76	<.0005*
	Coarse	51.02	32.47		
<b>90</b>	Ultrafine	297.86	67.92	11.54	<.0005
	Coarse	96.64	67.19		
<b>120</b>	Ultrafine	391.79	49.32	13.43	<.0005*
	Coarse	145.69	87.42		
<b>150</b>	Ultrafine	450.25	108.07	9.15	<.0005
	Coarse	196.02	107.24		
<b>180</b>	Ultrafine	477.14	151.41	6.41	<.0005
	Coarse	236.56	139.18		
*Based on Satterthwaite approximation					

### A. Ultrafine Silica



### B. Coarse Silica

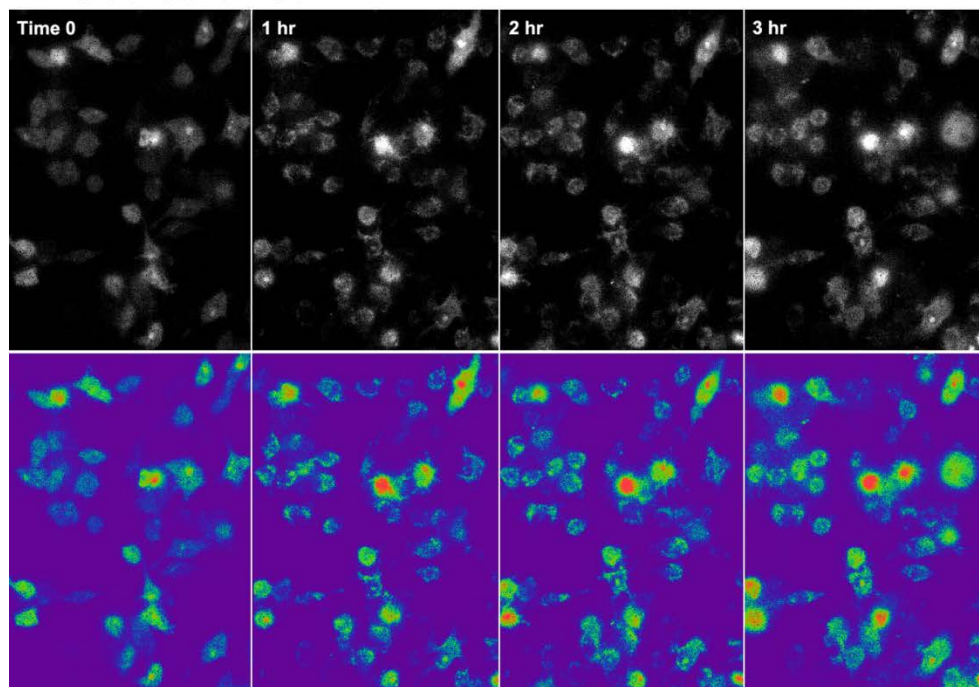


**Figure 18A: Representative images of the live cell experiment collected at 0, 1, 2 and 3 hours.**

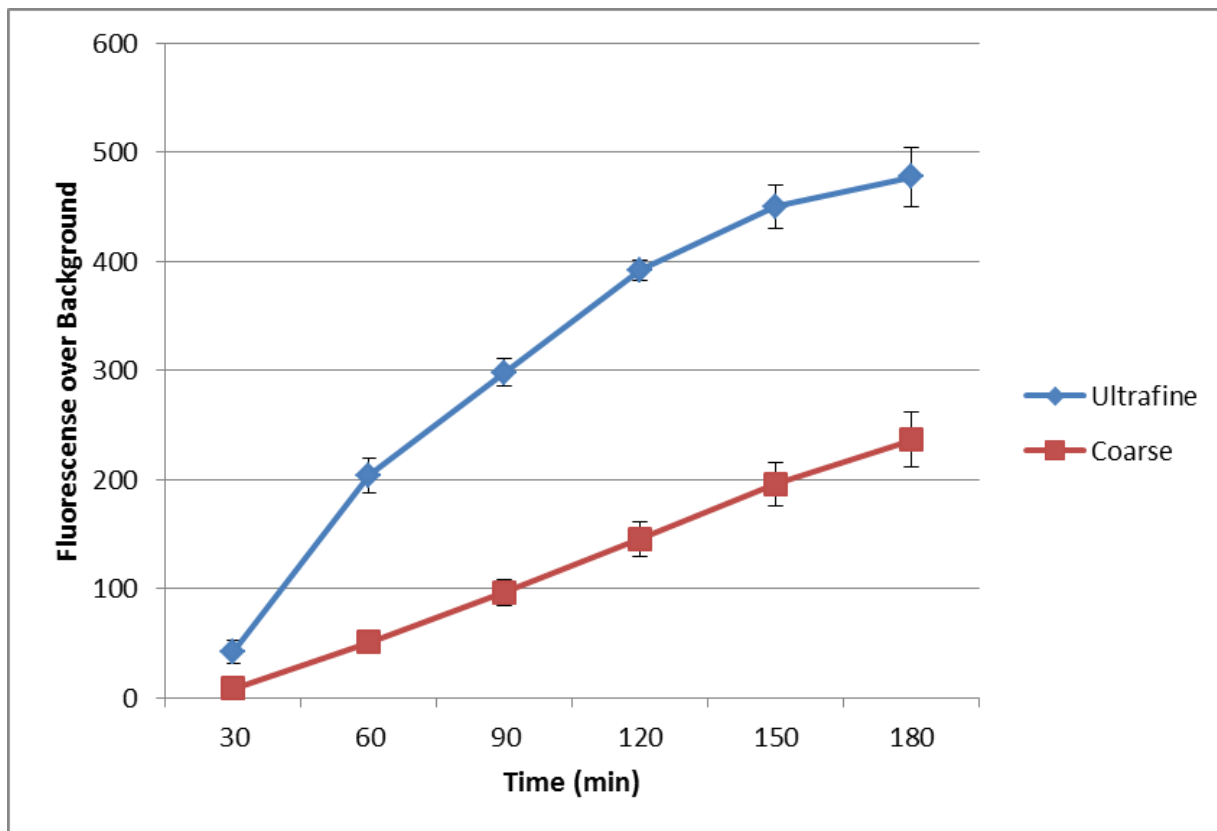


**Figure 18B: Increase in fluorescence over background resulting from exposure of RAW 264.7 cells to UF and C particles.**

As can be seen in Table 6, differences between the UF and C particle size conditions were significant at the 0.01 level for Period 1 and significant at the 0.001 level for all other periods. Mean fluorescence levels were consistently higher for samples exposed to UF particles. It can be seen in Figure 18 that fluorescence values increase over time in both conditions. However the increase appears to be both more gradual and more linear in samples exposed to C particles than in samples exposed to UF particles. This data corroborates what was seen in the TEM images since the PL formation should correspond to the mROS generation.

**Expression of Inflammatory cytokines:** As a way of elucidating the differences in expression of inflammatory cytokines based on exposure to different sized particles, we exposed AM to UF, S, R and C particles for two-, four- and eight-hour exposure periods. A Luminex 200

(Bio-Plex200, Bio-Rad) was used to measure the following cytokines in cell culture supernatant: FGF-basic (fibroblast growth factor 2), GM-CSF (granulocyte-macrophage colony-stimulating factor or colony stimulating factor 2), IFN- $\gamma$  (interferon-gamma), IL-1 $\alpha$ , IL-1 $\beta$ , KC (melanoma growth stimulating activity, alpha), IL2, IL4, IL5, IL6, IL10, IL12B, IL13, IL17A, IP-10 (CXCL10), MCP-1 (monocyte chemoattractant protein 1), MIP-1 alpha (macrophage inflammatory protein 1-alpha), MIG (CXCL9), TNF- $\alpha$  (tumor necrosis factor alpha), and VEGFA (vascular endothelial growth factor A). The data show that for each exposure period the positive control resulted in elevated expression of the measured cytokines when compared to the particles exposures and the negative controls.

The results from the Bio-Plex analysis for the two hour exposure period are shown for TNF- $\alpha$  in Figure 19A. For this exposure period each particle size showed a significant difference on expression of TNF- $\alpha$  when compared to the control; however, there was no significant difference on the expression of TNF- $\alpha$  based on particle size. Other cytokines measured in the media from the particle exposures included IL-5, IL-10, IP-10, MCP-1 and MIP-1A but no statistical difference based on particles size was found for any of these inflammatory cytokines.

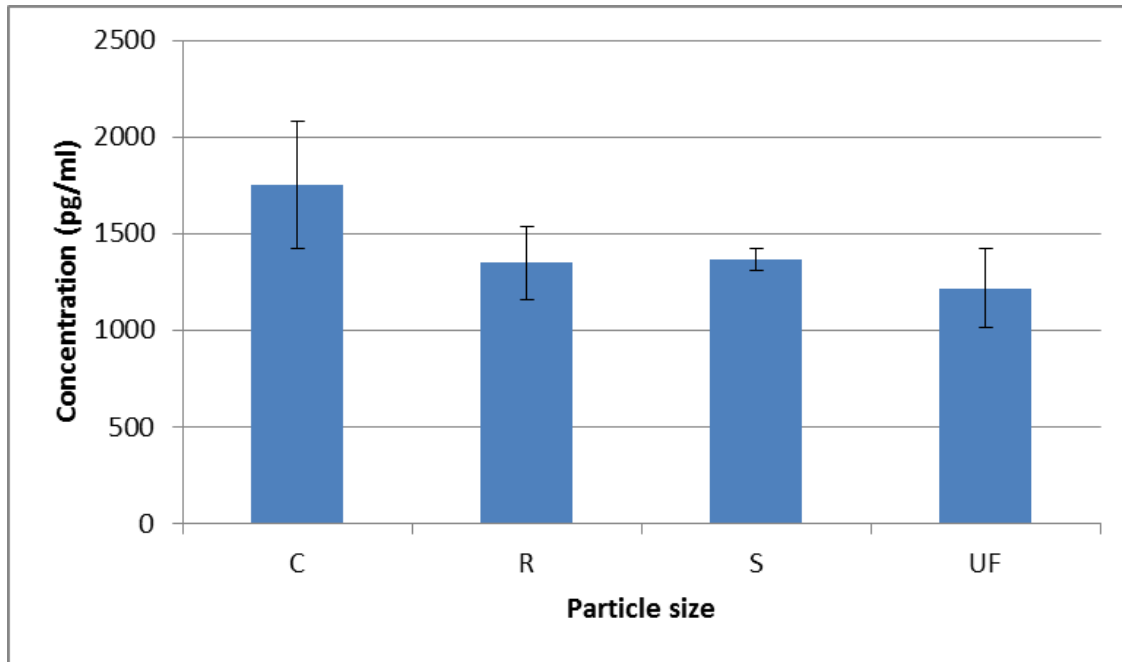
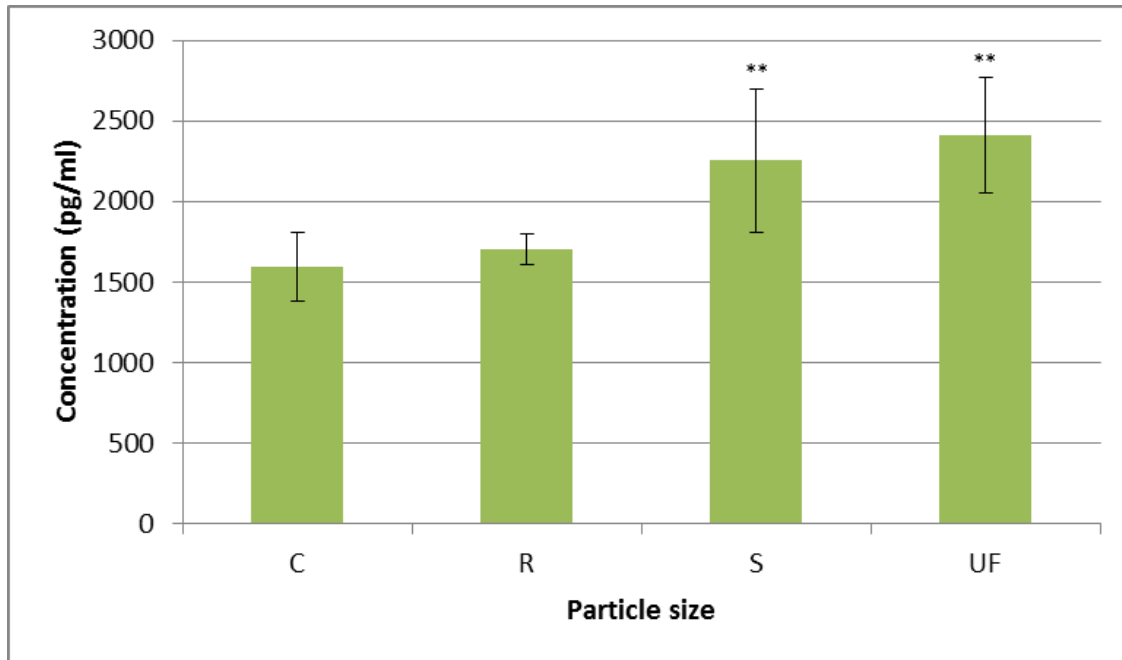


**Figure 19A: TNF- $\alpha$  expression after 2-hour exposure to four sizes of Crystalline Silica.**

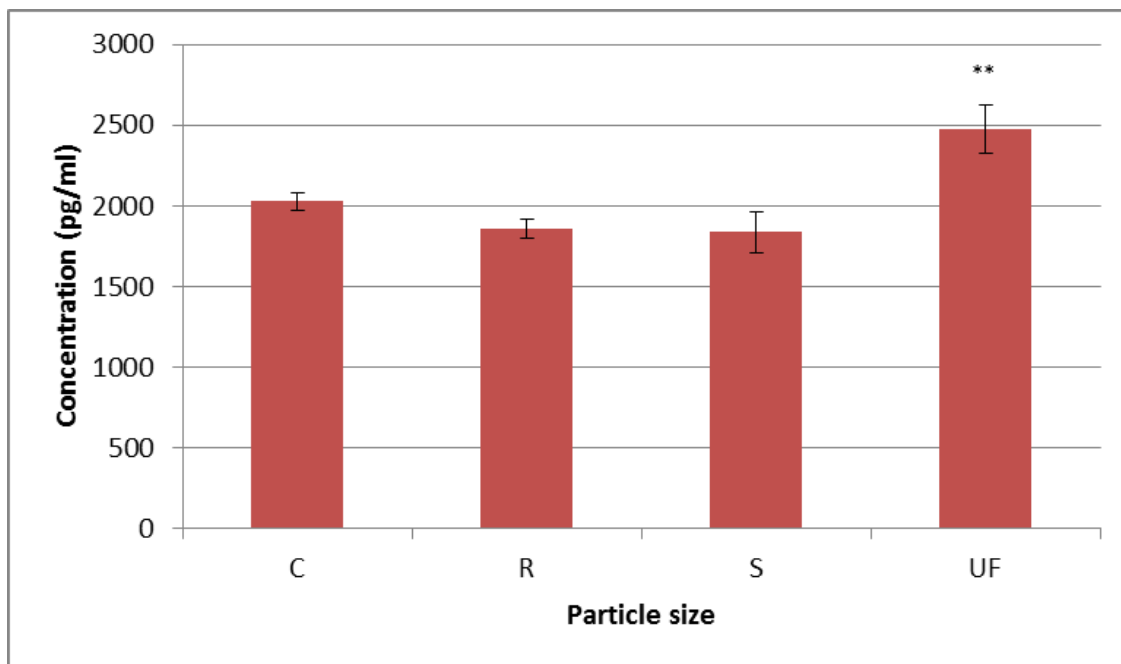
The results from the Bio-Plex analysis for the four hour exposure period are presented for TNF- $\alpha$  in Figure 19B. At this exposure period each particle size showed a significant difference on expression of TNF-alpha when compared to the control samples. In addition, both the UF and the S particles showed a statistically significant increase in expression of TNF- $\alpha$  when compared to both the C and R particles. Other cytokines measured during this analysis showing a significant difference of expression from exposure to UF versus C particles are; MCP-1(p-value = 0.07), IL-12 (p-value = 0.003), IL-5 (p-value = 0.002) and IL-6 (p-value = 0.013). These data also corroborate those seen in Figures 12 through 18, since the cytokine production would be expected to be delayed when compared to both PL formation and mROS generation.



\*\* Significant difference from C exposure at p-value = 0.005

**Figure 19B: TNF- $\alpha$  expression after 4-hour exposure to four sizes of Crystalline Silica.**

The results from the Bio-Plex analysis for the eight hour exposure period are presented for TNF- $\alpha$  in Figure 19C. At this exposure period, each particle size showed a significant difference on the expression of TNF- $\alpha$  when compared to the control samples. Also, the UF particles were found to significantly enhance the expression TNF- $\alpha$  when compared to the other three particle sizes. IL-5, IP-10, MCP-1 and MIP-1A were also measured in the particle expression media but no statistical difference based on particles size was found for any of these cytokines.



\*\* Significant difference from C exposure at p-value = 0.0001

**Figure 19C: TNF- $\alpha$  expression after 8-hour exposure to four sizes of Crystalline Silica.**

### 3.5 DISCUSSION

This study aimed at understanding the effect of different sized crystalline silica particles on the activation and response of murine alveolar macrophages. For this study, the CS was divided into four distinct size ranges, C (4  $\mu\text{m}$ ), R (2  $\mu\text{m}$ ), S (0.7  $\mu\text{m}$ ) and UF (0.3  $\mu\text{m}$ ), using a multi-cyclone sampling array. This method is capable of separating airborne occupational aerosols into distinct size ranges as described in the methods section. The particles at each size range were well defined both in the air and in the culture media. The results of this study show a consistent relationship between CS particle size and AM activation, as measured by TEM imaging, mROS generation, and inflammatory cytokine expression. The TEM data show that a greater number of UF particles are phagocytized in a shorter time period than C particles. In

addition, the number of PLs resulting from the UF exposure, the size of the PLs and the number of particles in each of the PLs is increased for the UF particles when compared to C particles. The mROS data show both a quicker and more intense response from exposure to UF particles versus C particles. Finally, the cytokine measurements show a significant increase in TNF- $\alpha$  expression from the AM at four- and eight-hour exposures. TNF- $\alpha$  expression is a primary indicator of AM activation (Huaux, 2007, Scarfi et al., 2009). Other cytokines measured during this analysis also show a significant difference between UF exposure versus C exposure at four hours, which include MCP-1, IL-12, IL-5 and IL-6. These results agree with previous work discussing cytokine release and AM activation due to silica exposure (Driscoll et al., 1995, Gozal et al., 2002, Balduzzi et al., 2004).

Much work, both in vivo and in vitro, is apparent in the literature comparing the effect of particle size on biological outcomes. This work usually agrees with our data that smaller particles create an enhanced biological response. Typically, this work uses engineered particles produced in laboratories at specific sizes, such as amorphous silica, titanium dioxide (TiO<sub>2</sub>) or gold (Winter et al., 2011, Downs et al., 2012, Leclerc et al., 2012, Sandberg et al., 2012). Oberdorster et al. observed significantly greater pulmonary inflammatory response to ultrafine (20 nm) TiO<sub>2</sub> in rats and mice when compared to larger particles (250 nm) (Oberdorster et al., 2000). Sager et al. found that ultrafine (21 nm) TiO<sub>2</sub> particles caused significantly greater inflammation and were more cytotoxic than fine (1  $\mu$ m) TiO<sub>2</sub> particles when instilled into rats (Sager et al., 2008). Also, Leclerc et al. investigated in vitro the rate of macrophage uptake and toxicity of fluorescent silica particles ranging from 850 nm to 150 nm and found that the smallest particles were internalized in greater quantities (Leclerc et al., 2012).

However, there are relatively few studies comparing biological effects from different sizes of crystalline silica. Wiessner et al. showed that a 1- $\mu\text{m}$  fraction was more lytic to red blood cell membranes than larger fractions; however, the larger size fractions resulted in a greater in vivo inflammatory response (Wiessner et al., 1989). In this study, the 1- $\mu\text{m}$  fraction was the smallest used. Kajiwara et al. demonstrated that 1.8  $\mu\text{m}$  size fraction more intensely effected the lungs of mice than a 0.7  $\mu\text{m}$  size fraction (Kajiwara et al., 2007). The major difference between our current study and these previous studies are the size ranges of the particles used for exposure and the procedure for separating the particles into these distinct size ranges. The particles sizes used in these studies ranged from 1.8  $\mu\text{m}$  to 0.7  $\mu\text{m}$  whereas the range for our study was 4  $\mu\text{m}$  to 0.3  $\mu\text{m}$ . Wang et al. showed that silica particles in the size fraction  $<200$  nm were both cytotoxic and genotoxic to human cells (Wang et al., 2007). However, this study did not compare the effects of particle size and did not use AM, so no activation criteria were reported.

Each of these previous studies used separation technologies that allowed particle crossover between size ranges such that smaller particles are present in larger particle range and vice versa. The biological effects measured in these experiments may have been influenced by the presence of these crossover particles. In the present study, the MCSA was used to separate the crystalline silica particles into distinct size ranges. The resulting particle size ranges are distinct with little crossover between ranges. In addition, the MCSA method allows for the particle separation to occur from the air in concentrations found in occupational environments. Because the particles are separated from the air, they are unaffected by the handling steps necessary for other separation techniques (Mischler et al., 2013).

In addition to showing the significance of particle size on the activation of AMs, our study also sheds some light on the molecular mechanisms behind this activation. The inflammatory effect was shown to be mediated from the recruitment of the NALP3 inflammasome (Cassel et al., 2008, Hornung et al., 2008, Dostert et al., 2008); however, the mechanism of this recruitment and silica-induced toxicity is still in question (Hamilton et al., 2008, Winter et al., 2011). In this study we provide data to indicate that mROS production occurs very early in the AM reaction to silica and coincides with the PL formation and swelling in the AM. In addition, the cytokine expression is delayed when compared to the mROS production. In our data, we see a significant difference in mROS generation based on exposure to UF particles versus C particles with the greatest difference between two and 2.5 hours. However, at the two hour time point we see no difference in cytokine expression between these particle sizes. By four hours, a significant difference in cytokine expression between the UF and C particle exposures appears. The TEM images show an increased number of UF particles being phagocytized at two hours and some swelling of the PLs is occurring. By the four hour time period, there are noticeably more PLs and they are noticeably swelling, when compared to the same time after C particle exposure and as the number of PLs increases the generation of mROS increases. Cassel et al. showed that cellular ROS signaling is occurring upstream of the NALP3 inflammasome activation. Dostert et al. suggested that these inflammasome activating cellular ROS are generated by NADPH oxidase complexes on the phagolysosome membrane (Dostert et al., 2008). This information, along with the data presented in this study, lends further definition to the pathway recently outlined by Lueng (Leung et al., 2012). In this process, cellular ROS is generated by both the mitochondria and the NADPH oxidase after phagocytosis and this process happens quickly after exposure. The cellular ROS then activates the NALP3 inflammasome

leading to expression of inflammatory cytokines. Our data supports this mechanism since the UF particles are more quickly incorporated into PLs, there are a greater number of PLs formed, corresponding to an increase in mROS generation and ultimately to elevated expression of inflammatory cytokines. Since only mROS was measured in this study, our data suggest that the increase in cellular ROS, as described earlier, is at least partly caused by generation of ROS in the mitochondria.

A second possibility resulting in inflammation is the activation of the NF $\kappa$ B pathway by cellular ROS. This pathway has been shown to be activated by CS (Fubini and Hubbard, 2003, Cox, 2011) resulting in the expression of TNF- $\alpha$ . Our data also supports this pathway, since TNF- $\alpha$  production continues to increase as the number of PLs and mROS generation increase in the AM. Scarfi et al. add a slightly different perspective on this mechanisms (Scarfi et al., 2009) by showing that cellular ROS generation and TNF- $\alpha$  expression occur in the absence of phagocytosis. In this case the plasma membrane appears to play a key role in the cellular ROS generation.

Taken together, these data suggest that two potential pathways, independent of each other, lead to the inflammatory response in AM. The first pathway was suggested by Scarfi et al. where the cellular ROS generation results from the CS interaction with the plasma membrane prior to phagocytosis, as a result of lipid peroxidation. Our data show mROS generation occurring with the introduction of the CS particles and TNF- $\alpha$  expression measured at two hours after exposure. In addition, our data show that the mROS production and TNF- $\alpha$  expression increase more quickly corresponding to an increase in the number of PLs formed. In this case, the mROS generation would result from the PL membrane disruption caused by CS and add to the cellular ROS generated from the plasma membrane. Since there are a greater number of PLs

created in response to the UF particle exposure, the difference in mROS generation between the two exposure scenarios, as well as the resulting TNF- $\alpha$  expression, should increase as the PLs are formed. This is exactly what our data show. In this slightly delayed scenario the inflammatory response would result from PL generated mROS either through the activation of the NALP3 inflammasome or through the initiation of the NF $\kappa$ B cascade. In both scenarios, the UF particles should cause an enhanced response due first from plasma membrane interaction with a larger number of CS particles and then from the formation of a greater number of PLs after phagocytosis.

This study has provided evidence that UF silica particles enhance the activation of AM when compared to larger silica particles usually represented in in vitro and in vivo research. However, these data are only meaningful if it can be shown that UF silica particles are a relevant occupational exposure. Recently it was shown that nanoparticles, ranging from 850 to 100 nm inhaled by rats were found in the alveolar macrophages of these animals (Morfeld et al., 2012) providing evidence that particles as small as 100 nm can be incorporated into AMs. Furthermore, it has been shown that in occupational environments there is significant variation in particle size and size-related silica content (Sirianni et al., 2008), and as the average particle size of the sample decreases, the percent silica of the sample may increase (Page, 2003). Because such substantial differences in particle size and CS content of occupational aerosols have been shown to occur and because we have shown in this study that UF CS particles enhance the activation of AM, compared to larger CS particles, more research is needed to more fully define this exposure and potential adverse biological outcomes of UF silica particles. In addition, the results of this study lend support to the growing chorus of researchers calling for regulations based on metrics capable of measuring UF and nanoparticles, to help better protect workers from this exposure.

## 4.0 CONCLUSIONS

Exposure of workers to crystalline silica in the US and worldwide has resulted in extensive disease and continues to be an occupational hazard for millions of workers (NIOSH, 2002, WHO, 2000). As a result of the mortality from this exposure, mass-based regulations were put in place in the US and these regulations had the result of steadily reducing the silicosis mortality. However, this decline in mortality has ceased and today silicosis results in 200 deaths per year in the US and this number has remained steady for the last decade even though (NIOSH, 2013) occupational exposure to CS, as measured using a mass-based metric, has remained at or below the regulated mass-exposure concentrations (Beaudry et al., 2013). One possible reason is the presence of very small particles that are not properly regulated by these mass-based standards. Even at mass-based concentrations which are below the regulatory standards, millions of ultrafine particles, with an aerodynamic diameter below 1  $\mu\text{m}$ , can be measured in the workplace (Oberdorster et al., 2005). If these particles create a similar or even more enhanced adverse biological reaction, when compared to larger particles, than the use of a mass-based standard would not be effective in mitigating this hazard. Occupational studies have been completed which show that these ultrafine particles can exist in numerous occupations where silica is a respiratory hazard (Sirianni et al., 2008, NIOSH, 2002), however, no methods exist that 1) can successfully separate these particles into distinct size ranges for toxicity evaluation and 2) are amenable for sampling in many work environments. As a result, no occupational studies have been completed evaluating both the size and size-related toxicity of these occupational CS particles. To that end this dissertation describes the design and evaluation of a method capable of overcoming the limitations that arise when attempting to collect sufficient

mass of ultrafine particles from an occupational or ambient environment, including; (1) the potential for a high mass concentration of the aerosol mixture, (2) the probability that the bigger particles will make-up a large percentage of the overall aerosol mass concentration, and the necessity of separating these particles while avoiding their inclusion in the smaller particle collection bins, and (3) the need for a compact and simple system that can be used in challenging occupational environments.

**Successful design of method to collect size selective occupational aerosols:** This study focused on the development and laboratory evaluation of a multi-cyclone sampling array, capable of separating occupational aerosols into distinct size ranges, over extended sampling periods to allow for collection of sufficient quantity of particles for toxicological testing and physical/chemical characterization. This novel measurement method was designed using a series of cyclones for collection of size-segregated particles. Cyclones have been widely used for size-selective particle sampling and have been demonstrated to have significant advantages over impactors for extended operation and high mass loadings (Kenny et al., 2004). The results presented here, using SMPS, APS, DLS/LLS and SEM/EDS data, show that this multi-cyclone system was able to successfully collect distinct size-segregated particles at appropriate masses to perform toxicological sampling (Chapter 2). In addition, the size and simplicity of the MCAS method makes it feasible for occupational sampling. For example, this method is currently being used by the Aerosol and Toxic Substances group at the Office of Mine Safety and Health Research, in underground mines to successfully collect size segregated samples for toxicological evaluations and physical/chemical characterization.

Although this research focused on crystalline silica, this sampling method can be used for size-segregated sampling of a wide variety of occupational or environmental aerosols. Because this method allows for the concurrent collection of four different sizes of aerosols, it enables scientists to conduct physical and chemical evaluations, as well as *in vivo* or *in vitro* evaluations, of these simultaneously collected aerosols.

Chapter 2 presents results confirming the ability of the MCAS method to successfully collect size-segregated particles. However, it was also necessary to evaluate whether the particles collected by the MCAS can be successfully used in toxicity studies and if the collection of these size-segregated silica particles is important, based on biological outcomes. Much information has been presented in the literature showing enhanced biological response of nano- or ultrafine particles when compared to larger particles (Oberdorster et al., 2005). However, most of this *in vitro* work has been completed using engineered nano- and ultrafine particles, such as amorphous silica, titanium dioxide (TiO<sub>2</sub>) or gold, which were created in the laboratory (Winter et al., 2011, Downs et al., 2012, Leclerc et al., 2012, Sandberg et al., 2012). Little work has been done on crystalline silica, and the few studies addressing this issue either used a separation technology which allowed crossover between the particles size ranges or did not complete a direct comparison between smaller and larger particles. Thus chapter 3 of this dissertation presents a study comparing the effects of different sized silica particles, collected using the MCAS method, on the activation of macrophages. This study has a two-fold purpose; 1) to evaluate if nano- and ultrafine silica particles (<300 nm) are more effective at activating macrophages, and 2) to assess the ability of the particles collected by the MCAS to be used in these toxicological studies.

**Small particles are more affective and initiating the inflammatory response in murine alveolar macrophages:** This study has provided evidence that UF silica particles enhance the activation of AM when compared to larger silica particles usually represented in in vitro and in vivo research. These data identified differences in particle uptake and formation of subcellular organelles based on particle size. In addition, these data show that the smallest particles, with a geometric mean of 0.3  $\mu\text{m}$ , significantly increase the generation of mitochondrial ROS and the expression of cytokines when compared to larger crystalline silica particles, with a geometric mean of 4.1  $\mu\text{m}$ .

However, these data are only meaningful if it can be shown that UF silica particles are a relevant occupational exposure. Modeling studies have shown that as the particle size decreases, the fraction of particles deposited in the lung increases, in both human and animal models (Martin et al., 2008, Weers et al., 2009, Kuehl et al., 2012). Recently it was shown that nanoparticles, ranging from 850 to 100 nm inhaled by rats were found in the alveolar macrophages of these animals (Morfeld et al., 2012) providing evidence that particles as small as 100 nm can be incorporated into AMs.

Also, it has been shown that in occupational environments there is significant variation in particle size and size-related silica content (Sirianni et al., 2008), and as the average particle size of the sample decreases, the percent silica of some samples increase (Page, 2003). All of this data suggests that small (300 nm) CS particles are both present in occupational environments and can be incorporated in the AM based on airborne exposure to these particles. As particles size decreases there is a corresponding increase in particle number (Oberdorster et al., 2005) per mass unit. At particle concentrations in air below established mass-based exposure levels, very high particle number concentrations - up to  $10^6 \text{cm}^{-3}$  in occupational environments and  $10^4 \text{cm}^{-3}$  in

ambient air - exist (Bugarski et al., 2009, Hughes LS, 1998) , and this high number concentration is likely to result in toxicological effects, even at low ambient mass concentrations (Oberdorster et al., 2005). Thus exposure to ultrafine and nano-particles presents the potential for the occupational exposure to these particles to be below the mass-based regulatory levels yet still result in negative health effects in the exposed worker. To our knowledge this is the first method that has been shown to successfully separate airborne crystalline silica into distinct size groups. Because these UF CS particles are potentially underrepresented by the occupational mass-based standards, then this research is the initial step in evaluating whether these mass-based standards need adjusting when related to CS exposure.

**Future direction:** This study has offered the hypothesis that UF particles generate ROS from both contact with the plasma membrane and from the increased formation of PL's within the AM. After this initial reaction, the silica induced apoptosis will occur releasing these particles to initiate another cycle of phagocytosis and inflammation. In this case, UF particles will cause a perpetually enhanced silica/AM cycle leading to elevated levels of ROS, TNF- $\alpha$  and other inflammatory cytokines and apoptosis (Wang et al., 2007), and eventual damage to lung tissue and epithelial hyperplasia (Cox, 2011), potentially resulting in a quicker onset of fibrosis. Recently, an increase and severity of rapid progressive massive fibrosis has been reported (Laney et al., 2010). Our data supports the possibility of quicker onset of fibrosis as the size of the CS particles decrease, potentially resulting from the use of newer mining technology in thinner coal seams. If UF particles are present in this occupational environment and we have already shown that these UF particles create an enhanced AM response, than we can hypothesis that an increase

in the concentration of UF particles is resulting in the development of this recent trend of early onset massive progressive fibrosis. This hypothesis could be investigated in future projects.

In addition, because such substantial differences in particle size and CS content of occupational aerosols have been shown to occur, more research is needed to more fully define the UF CS exposure and to understand the molecular mechanisms that result in this enhanced response.

Finally, the results of this study lend support to the growing chorus of researchers calling for regulations based on metrics capable of measuring UF and nanoparticles, to help better protect workers from this exposure. More research to evaluate the effectiveness of additional exposure metrics, such as surface area measurements or particle number concentration, is necessary to help reduce this occupational exposure and the resulting disease.

## BIBLIOGRAPHY

- 29 CFR PART 1926 SUBPART D Safety and Health Regulations for Construction. *In:* OCCUPATIONAL SAFETY AND HEALTH ADMINISTRATION, C. O. F. R. (ed.). Washington DC: US Government Printing Office, Office of the Federal Register.
- 30 CFR PART 70 Dust Standards, Mandatory Health Standards, Underground Coal Mines,. *In:* MINE SAFETY AND HEALTH ADMINISTRATION & CODE OF FEDERAL REGULATIONS (eds.). Washington DC: US Government Printing Office, Office of the Federal Register.
- 40 CFR PART 50 NATIONAL PRIMARY AND SECONDARY AMBIENT AIR QUALITY STANDARDS. *In:* US DEPARTMENT OF THE INTERIOR, E. P. A., CODE OF FEDERAL REGULATIONS, (ed.). Washington DC: US Government Printing Office, Office of the Federal Register.
- BALDUZZI, M., DIOCIAIUTI, M., DE BERARDIS, B., PARADISI, S. & PAOLETTI, L. 2004. In vitro effects on macrophages induced by noncytotoxic doses of silica particles possibly relevant to ambient exposure. *Environ Res*, 96, 62-71.
- BEAUDRY, C., LAVOUE, J., SAUVE, J. F., BEGIN, D., SENHAJI RHAZI, M., PERRAULT, G., DION, C. & GERIN, M. 2013. Occupational exposure to silica in construction workers: a literature-based exposure database. *J Occup Environ Hyg*, 10, 71-7.
- BODO, M., MUZI, G., BELLUCCI, C., LILLI, C., CALVITTI, M., LUMARE, A., DELL'OMO, M., GAMBELUNGHE, A., BARONI, T. & MURGIA, N. 2007. Comparative in vitro studies on the fibrogenic effects of two samples of silica on epithelial bronchial cells. *J Biol Regul Homeost Agents*, 21, 97-104.
- BROOK, R. D., RAJAGOPALAN, S., POPE, C. A., BROOK, J. R., BHATNAGAR, A., DIEZ-ROUX, A. V., HOGUIN, F., HONG, Y., LUEPKER, R. V., MITTLEMAN, M. A., PETERS, A., SISCOVICK, D., SMITH, S. C., WHITSEL, L. & KAUFMAN, J. D. 2010. Particulate Matter Air Pollution and Cardiovascular Disease: An Update to the Scientific Statement from the American Heart Association. *Circulation*, 2331-2378.
- BUGARSKI, A. D., SCHNAKENBERG, G. H., JR., HUMMER, I. A., CAUDA, E., JANISKO, S. I. & PATTS, L. D. 2009. Effects of diesel exhaust aftertreatment devices on concentrations and size distribution of aerosols in underground mine air. *Environ Sci Technol*, 43, 6737-43.
- CASSEL, S. L., EISENBARTH, S. C., IYER, S. S., SADLER, J. J., COLEGIO, O. R., TEPHLY, L. A., CARTER, A. B., ROTHMAN, P. B., FLAVELL, R. A. & SUTTERWALA, F. S. 2008. The Nalp3 inflammasome is essential for the development of silicosis. *Proc Natl Acad Sci U S A*, 105, 9035-40.
- CENTERS FOR DISEASE, C. & PREVENTION 2005. Silicosis mortality, prevention, and control--United States, 1968-2002. *MMWR Morb Mortal Wkly Rep*, 54, 401-5.
- CHURG, A. & BRAUER, M. 2000. Ambient atmospheric particles in the airways of human lungs. *Ultrastruct Pathol*, 24, 353-61.

- COX, L. A., JR. 2011. An exposure-response threshold for lung diseases and lung cancer caused by crystalline silica. *Risk Anal*, 31, 1543-60.
- DONALDSON, K. & MACNEE, W. 2001. Potential mechanisms of adverse pulmonary and cardiovascular effects of particulate air pollution (PM10). *Int J Hyg Environ Health*, 203, 411-5.
- DOSTERT, C., PETRILLI, V., VAN BRUGGEN, R., STEELE, C., MOSSMAN, B. T. & TSCHOPP, J. 2008. Innate immune activation through Nalp3 inflammasome sensing of asbestos and silica. *Science*, 320, 674-7.
- DOWNES, T. R., CROSBY, M. E., HU, T., KUMAR, S., SULLIVAN, A., SARLO, K., REEDER, B., LYNCH, M., WAGNER, M., MILLS, T. & PFUHLER, S. 2012. Silica nanoparticles administered at the maximum tolerated dose induce genotoxic effects through an inflammatory reaction while gold nanoparticles do not. *Mutat Res*, 745, 38-50.
- DRISCOLL, K. E., HASSENBEIN, D. G., CARTER, J. M., KUNKEL, S. L., QUINLAN, T. R. & MOSSMAN, B. T. 1995. TNF alpha and increased chemokine expression in rat lung after particle exposure. *Toxicol Lett*, 82-83, 483-9.
- FUBINI, B. & HUBBARD, A. 2003. Reactive oxygen species (ROS) and reactive nitrogen species (RNS) generation by silica in inflammation and fibrosis. *Free Radic Biol Med*, 34, 1507-16.
- GOZAL, E., ORTIZ, L. A., ZOU, X., BUROW, M. E., LASKY, J. A. & FRIEDMAN, M. 2002. Silica-induced apoptosis in murine macrophage: involvement of tumor necrosis factor-alpha and nuclear factor-kappaB activation. *Am J Respir Cell Mol Biol*, 27, 91-8.
- GREENBERG, M. I., WAKSMAN, J. & CURTIS, J. 2007. Silicosis: a review. *Dis Mon*, 53, 394-416.
- HALL, R. M., ACHUTAN, C., SOLLBERGER, R., MCCLEERY, R. E. & RODRIGUEZ, M. 2013. Exposure assessment for roofers exposed to silica during installation of roof tiles. *J Occup Environ Hyg*, 10, D6-10.
- HAMILTON, R. F., JR., THAKUR, S. A. & HOLIAN, A. 2008. Silica binding and toxicity in alveolar macrophages. *Free Radic Biol Med*, 44, 1246-58.
- HINDS, W. C. 1999. *Aerosol Technology: Properties, behavior and measurement of airborne particles*, John Wiley & Sons.
- HORNUNG, V., BAUERNFEIND, F., HALLE, A., SAMSTAD, E. O., KONO, H., ROCK, K. L., FITZGERALD, K. A. & LATZ, E. 2008. Silica crystals and aluminum salts activate the NALP3 inflammasome through phagosomal destabilization. *Nat Immunol*, 9, 847-56.
- HUAUX, F. 2007. New developments in the understanding of immunology in silicosis. *Curr Opin Allergy Clin Immunol*, 7, 168-73.
- HUGHES LS, C. G., GONE J , AMES M ,OLMEZ I. 1998. Physical and chemical characterization of atmospheric ultrafine particles in the Los Angeles area. *Environ Sci Technol* 32, 1153-1161.
- KAJIWARA, T., OGAMI, A., YAMATO, H., OYABU, T., MORIMOTO, Y. & TANAKA, I. 2007. Effect of particle size of intratracheally instilled crystalline silica on pulmonary inflammation. *J Occup Health*, 49, 88-94.
- KENNY, L. C., GUSSMAN, R. & MEYER, M. 2000. Development of a sharp-cut cyclone for ambient aerosol monitoring applications (vol 32, pg 338, 2000). *Aerosol Science and Technology*, 32, 613-616.
- KENNY, L. C. & GUSSMAN, R. A. 1997. Characterization and modelling of a family of cyclone aerosol pre-separators. *Journal of Aerosol Science*, 28, 677-688.

- KENNY, L. C., MERRIFIELD, T., MARK, D., GUSSMAN, R. & THORPE, A. 2004. The development and designation testing of a new USEPA-approved fine particle inlet: A study of the USEPA designation process. *Aerosol Science and Technology*, 38, 15-22.
- KIM, S., JAQUES, P. A., CHANG, M. C., BARONE, T., XIONG, C., FRIEDLANDER, S. K. & SIOUTAS, C. 2001a. Versatile aerosol concentration enrichment system (VACES) for simultaneous in vivo and in vitro evaluation of toxic effects of ultrafine, fine and coarse ambient particles - Part II: Field evaluation. *Journal of Aerosol Science*, 32, 1299-1314.
- KIM, S., JAQUES, P. A., CHANG, M. C., FROINES, J. R. & SIOUTAS, C. 2001b. Versatile aerosol concentration enrichment system (VACES) for simultaneous in vivo and in vitro evaluation of toxic effects of ultrafine, fine and coarse ambient particles - Part I: Development and laboratory characterization. *Journal of Aerosol Science*, 32, 1281-1297.
- KNOL, A. B., DE HARTOG, J. J., BOOGAARD, H., SLOTTJE, P., VAN DER SLUIJS, J. P., LEBRET, E., CASSEE, F. R., WARDEKKER, J. A., AYRES, J. G., BORM, P. J., BRUNEKREEF, B., DONALDSON, K., FORASTIERE, F., HOLGATE, S. T., KREYLING, W. G., NEMERY, B., PEKKANEN, J., STONE, V., WICHMANN, H. E. & HOEK, G. 2009. Expert elicitation on ultrafine particles: likelihood of health effects and causal pathways. *Part Fibre Toxicol*, 6, 19.
- KROEMER, G. & JAATTELA, M. 2005. Lysosomes and autophagy in cell death control. *Nat Rev Cancer*, 5, 886-97.
- KUEHL, P. J., ANDERSON, T. L., CANDELARIA, G., GERSHMAN, B., HARLIN, K., HESTERMAN, J. Y., HOLMES, T., HOPPIN, J., LACKAS, C., NORENBURG, J. P., YU, H. & MCDONALD, J. D. 2012. Regional particle size dependent deposition of inhaled aerosols in rats and mice. *Inhal Toxicol*, 24, 27-35.
- LANEY, A. S., PETSONK, E. L. & ATTFIELD, M. D. 2010. Pneumoconiosis among underground bituminous coal miners in the United States: is silicosis becoming more frequent? *Occup Environ Med*, 67, 652-6.
- LECLERC, L., RIMA, W., BOUDARD, D., POURCHEZ, J., FOREST, V., BIN, V., MOWAT, P., PERRIAT, P., TILLEMENT, O., GROSSEAU, P., BERNACHE-ASSOLLANT, D. & COTTIER, M. 2012. Size of submicrometric and nanometric particles affect cellular uptake and biological activity of macrophages in vitro. *Inhal Toxicol*, 24, 580-8.
- LEUNG, C. C., YU, I. T. & CHEN, W. 2012. Silicosis. *Lancet*, 379, 2008-18.
- LI, N., SIOUTAS, C., CHO, A., SCHMITZ, D., MISRA, C., SEMPFF, J., WANG, M., OBERLEY, T., FROINES, J. & NEL, A. 2003. Ultrafine particulate pollutants induce oxidative stress and mitochondrial damage. *Environ Health Perspect*, 111, 455-60.
- MARPLE, V., RUBOW, KL. 1983. An aerosol chamber for instrument evaluation and calibration. *Am Ind Hyg Assoc J*, 44, 7.
- MARTIN, A. R., THOMPSON, R. B. & FINLAY, W. H. 2008. MRI measurement of regional lung deposition in mice exposed nose-only to nebulized superparamagnetic iron oxide nanoparticles. *J Aerosol Med Pulm Drug Deliv*, 21, 335-42.
- MAYNARD, A. D. & AITKEN, R. J. 2007. Assessing exposure to airborne nanomaterials: Current abilities and future requirements. *Nanotoxicology*, 1, 26-41.
- MAYNARD, A. D. & KENNY, L. C. 1995. Performance Assessment of 3 Personal Cyclone Models, Using an Aerodynamic Particle Sizer. *Journal of Aerosol Science*, 26, 671-684.
- MCKINNEY, W., CHEN, B., SCHWEGLER-BERRY, D. & FRAZER, D. G. 2013. Computer-automated silica aerosol generator and animal inhalation exposure system. *Inhal Toxicol*, 25, 363-72.

- MISCHLER, S. E., CAUDA, E. G., DI GIUSEPPE, M. & ORTIZ, L. A. 2013. A multi-cyclone sampling array for the collection of size-segregated occupational aerosols. *J Occup Environ Hyg*, 10, 685-93.
- MONTEILLER, C., TRAN, L., MACNEE, W., FAUX, S., JONES, A., MILLER, B. & DONALDSON, K. 2007. The pro-inflammatory effects of low-toxicity low-solubility particles, nanoparticles and fine particles, on epithelial cells in vitro: the role of surface area. *Occup Environ Med*, 64, 609-15.
- MORFELD, P., TREUMANN, S., MA-HOCK, L., BRUCH, J. & LANDSIEDEL, R. 2012. Deposition behavior of inhaled nanostructured TiO<sub>2</sub> in rats: fractions of particle diameter below 100 nm (nanoscale) and the slicing bias of transmission electron microscopy. *Inhal Toxicol*, 24, 939-51.
- MOSSMAN, B. T. & CHURG, A. 1998. Mechanisms in the pathogenesis of asbestosis and silicosis. *Am J Respir Crit Care Med*, 157, 1666-80.
- MURDOCK, R. C., BRAYDICH-STOLLE, L., SCHRAND, A. M., SCHLAGER, J. J. & HUSSAIN, S. M. 2008. Characterization of nanomaterial dispersion in solution prior to in vitro exposure using dynamic light scattering technique. *Toxicol Sci*, 101, 239-53.
- NATIONAL INSTITUTE FOR OCCUPATIONAL SAFETY AND HEALTH 2002. NIOSH HAZARD REVIEW: Health Effects of Occupational Exposure to Respirable Crystalline Silica. In: DEPARTMENT OF HEALTH AND HUMAN SERVICES (ed.).
- NIOSH 2002. NIOSH Hazard Review; Health Effects of Occupational Exposure to Respirable Crystalline Silica. Department of Health and Human Services, CDC, NIOSH, Publication NO.2002-129.
- NIOSH. 2013. *Work-Related Lung Disease Surveillance System (eWoRLD); Silicosis Mortality* [Online]. NIOSH. Available: <http://www2a.cdc.gov/drds/worldreportdata/SubsectionDetails.asp?ArchiveID=1&SubsectionTitleID=8> [Accessed August 6 2013].
- OBERDORSTER, G., FINKELSTEIN, J. N., JOHNSTON, C., GELEIN, R., COX, C., BAGGS, R. & ELDER, A. C. 2000. Acute pulmonary effects of ultrafine particles in rats and mice. *Res Rep Health Eff Inst*, 5-74; disc 75-86.
- OBERDORSTER, G., OBERDORSTER, E. & OBERDORSTER, J. 2005. Nanotoxicology: an emerging discipline evolving from studies of ultrafine particles. *Environ Health Perspect*, 113, 823-39.
- PAGE, S. J. 2003. Comparison of coal mine dust size distributions and calibration standards for crystalline silica analysis. *AIHA J (Fairfax, Va)*, 64, 30-9.
- PAGE, S. J. & VOLKWEIN, J. C. 2009. A revised conversion factor relating respirable dust concentrations measured by 10 mm Dorr-Oliver nylon cyclones operated at 1.7 and 2.0 L min<sup>-1</sup>. *J Environ Monit*, 11, 684-9.
- PAUR, H. R., CASSEE, F. R., TEEGUARDEN, J., FISSAN, H., DIABATE, S., AUFDERHEIDE, M., KREYLING, W. G., HANNINEN, O., KASPER, G., RIEDIKER, M., ROTHEN-RUTISHAUSER, B. & SCHMID, O. 2011. In-vitro cell exposure studies for the assessment of nanoparticle toxicity in the lung-A dialog between aerosol science and biology. *Journal of Aerosol Science*, 42, 668-692.
- POPE, C. A., 3RD, BURNETT, R. T., KREWSKI, D., JERRETT, M., SHI, Y., CALLE, E. E. & THUN, M. J. 2009. Cardiovascular mortality and exposure to airborne fine particulate matter and cigarette smoke: shape of the exposure-response relationship. *Circulation*, 120, 941-8.

- POPE, C. A., MUHLESTEIN, J. B., MAY, H. T., RENLUND, D. G., ANDERSON, J. L. & HORNE, B. D. 2006. Ischemic Heart Disease Events Triggered by Short-Term Exposure to Fine Particulate Air Pollution. *Circulation*, 2443-2448.
- PRISTINSKI, D. & CHASTEK, T. Q. 2009. A versatile, low-cost approach to dynamic light scattering. *Measurement Science & Technology*, 20.
- RAMGOLAM, K., FAVEZ, O., CACHIER, H., GAUDICHET, A., MARANO, F., MARTINON, L. & BAEZA-SQUIBAN, A. 2009. Size-partitioning of an urban aerosol to identify particle determinants involved in the proinflammatory response induced in airway epithelial cells. *Part Fibre Toxicol*, 6, 10.
- RIMAL, B., GREENBERG, A. K. & ROM, W. N. 2005. Basic pathogenetic mechanisms in silicosis: current understanding. *Curr Opin Pulm Med*, 11, 169-73.
- ROBINSON, K. M., JANES, M. S. & BECKMAN, J. S. 2008. The selective detection of mitochondrial superoxide by live cell imaging. *Nature Protocols*, 3, 941-947.
- ROSNER, B. 1990. *Fundamentals of Biostatistics, Third Edition*, Boston, Massachusetts, PWS-Kent Publishing Company.
- RUUSUNEN, J., TAPANAINEN, M., SIPPULA, O., JALAVA, P. I., LAMBERG, H., NUUTINEN, K., TISSARI, J., IHALAINEN, M., KUUSPALO, K., MAKI-PAKKANEN, J., HAKULINEN, P., PENNANEN, A., TEINILA, K., MAKKONEN, U., SALONEN, R. O., HILLAMO, R., HIRVONEN, M. R. & JOKINIEMI, J. 2011. A novel particle sampling system for physico-chemical and toxicological characterization of emissions. *Anal Bioanal Chem*, 401, 3183-95.
- SAGER, T. M., KOMMINENI, C. & CASTRANOVA, V. 2008. Pulmonary response to intratracheal instillation of ultrafine versus fine titanium dioxide: role of particle surface area. *Part Fibre Toxicol*, 5, 17.
- SANDBERG, W. J., LAG, M., HOLME, J. A., FRIEDE, B., GUALTIERI, M., KRUSZEWSKI, M., SCHWARZE, P. E., SKULAND, T. & REFSNES, M. 2012. Comparison of non-crystalline silica nanoparticles in IL-1beta release from macrophages. *Part Fibre Toxicol*, 9, 32.
- SARNAT, J. A., KOUTRAKIS, P. & SUH, H. H. 2000. Assessing the relationship between personal particulate and gaseous exposure of senior citizens living in Baltimore, MD. *J Air and Waste Management Association*, 1184-1198.
- SAUVE, J. F., BEAUDRY, C., BEGIN, D., DION, C., GERIN, M. & LAVOUE, J. 2013. Silica exposure during construction activities: statistical modeling of task-based measurements from the literature. *Ann Occup Hyg*, 57, 432-43.
- SCARFI, S., MAGNONE, M., FERRARIS, C., POZZOLINI, M., BENVENUTO, F., BENATTI, U. & GIOVINE, M. 2009. Ascorbic acid pre-treated quartz stimulates TNF-alpha release in RAW 264.7 murine macrophages through ROS production and membrane lipid peroxidation. *Respir Res*, 10, 25.
- SILLANPAA, M., HILLAMO, R., MAKELA, T., PENNANEN, A. S. & SALONEN, R. O. 2003. Field and laboratory tests of a high volume cascade impactor. *Journal of Aerosol Science*, 34, 485-500.
- SILVERMAN, D. T., SAMANIC, C. M., LUBIN, J. H., BLAIR, A. E., STEWART, P. A., VERMEULEN, R., COBLE, J. B., ROTHMAN, N., SCHLEFF, P. L., TRAVIS, W. D., ZIEGLER, R. G., WACHOLDER, S. & ATTFIELD, M. D. 2012. The Diesel Exhaust in Miners Study: A Nested Case-Control Study of Lung Cancer and Diesel Exhaust. *J National Cancer Institute*, 104, 855-868.

- SIRIANNI, G., HOSGOOD, H. D., 3RD, SLADE, M. D. & BORAK, J. 2008. Particle size distribution and particle size-related crystalline silica content in granite quarry dust. *J Occup Environ Hyg*, 5, 279-85.
- STEENHOF, M., GOSENS, I., STRAK, M., GODRI, K. J., HOEK, G., CASSEE, F. R., MUDWAY, I. S., KELLY, F. J., HARRISON, R. M., LEBRET, E., BRUNEKREEF, B., JANSSEN, N. A. & PIETERS, R. H. 2011. In vitro toxicity of particulate matter (PM) collected at different sites in the Netherlands is associated with PM composition, size fraction and oxidative potential--the RAPTES project. *Part Fibre Toxicol*, 8, 26.
- STEPHANIE, V., MARTINON, L., CACHIER, H., YAHYAOU, A., MARFAING, H. & BAEZA-SQUIBAN, A. 2011. Role of size and composition of traffic and agricultural aerosols in the molecular responses triggered in airway epithelial cells. *Inhal Toxicol*, 23, 627-40.
- STEPHANIE, V. M. L., CACHIER HELENE, YAHYAOU ABDERRAZAK, MARFAING HELENE, BAEZA-SQUIBAN ARMELLE 2011. Role of size and composition of traffic and agricultural aerosols in the molecular responses triggered in airway epithelial cells. *Inhalation Toxicology*, 23, 627-640.
- STERN, S. T., ADISESHIAH, P. P. & CRIST, R. M. 2012. Autophagy and lysosomal dysfunction as emerging mechanisms of nanomaterial toxicity. *Particle and Fibre Toxicology*, 9.
- THIBODEAU, M. S., GIARDINA, C., KNECHT, D. A., HELBLE, J. & HUBBARD, A. K. 2004. Silica-induced apoptosis in mouse alveolar macrophages is initiated by lysosomal enzyme activity. *Toxicol Sci*, 80, 34-48.
- THOMAS, J. C. 1987. The Determination of Log Normal Particle-Size Distributions by Dynamic Light-Scattering. *Journal of Colloid and Interface Science*, 117, 187-192.
- TSI, I. 2012a. Aerodynamic Particle Sizer Model 3321: Theory of Operation.
- TSI, I. 2012b. Scanning Mobility Particle Sizer™ Spectrometer (smps) Model 3936: Highly accurate, real-time nanoparticle sizing systems you can rely on for years.
- VANDERPOOL, R. W., PETERS, T. M., NATARAJAN, S., GEMMILL, D. B. & WIENER, R. W. 2001. Evaluation of the loading characteristics of the EPA WINSPM2.5 separator. *Aerosol Science and Technology*, 34, 444-456.
- VIRTANEN, A., JOUTSENSAARI, J., KOOP, T., KANNOSTO, J., YLI-PIRILA, P., LESKINEN, J., MAKELA, J. M., HOLOPAINEN, J. K., POSCHL, U., KULMALA, M., WORSNOP, D. R. & LAAKSONEN, A. 2010. An amorphous solid state of biogenic secondary organic aerosol particles. *Nature*, 467, 824-7.
- VOLKWEIN, J. C., ROBERT P. VINSON, LINDA J. MCWILLIAMS, DONALD P. TUCHMAN, STEVEN E. MISCHLER 2004. Performance of a New Personal REspirable Dust Monitor for Mine Use. *In: HHS CDC NATIONAL INSTITUTE FOR OCCUPATIONAL SAFETY AND HEALTH* (ed.).
- WANG, J. J., SANDERSON, B. J. & WANG, H. 2007. Cytotoxicity and genotoxicity of ultrafine crystalline SiO<sub>2</sub> particulate in cultured human lymphoblastoid cells. *Environ Mol Mutagen*, 48, 151-7.
- WATERS, K. M., MASIELLO, L. M., ZANGAR, R. C., TARASEVICH, B. J., KARIN, N. J., QUESENBERRY, R. D., BANDYOPADHYAY, S., TEEGUARDEN, J. G., POUNDS, J. G. & THRALL, B. D. 2009. Macrophage responses to silica nanoparticles are highly conserved across particle sizes. *Toxicol Sci*, 107, 553-69.

- WEERS, J., METZHEISER, B., TAYLOR, G., WARREN, S., MEERS, P. & PERKINS, W. R. 2009. A gamma scintigraphy study to investigate lung deposition and clearance of inhaled amikacin-loaded liposomes in healthy male volunteers. *J Aerosol Med Pulm Drug Deliv*, 22, 131-8.
- WHO. 2000. *Silicosis Fact Sheet N° 238* [Online]. Available: [http://www.who.int/peh/Occupational\\_health/OCHweb/OSHpages/OSHDdocuments/Factsheets/Silicosis.htm](http://www.who.int/peh/Occupational_health/OCHweb/OSHpages/OSHDdocuments/Factsheets/Silicosis.htm) [Accessed August 6 2013].
- WHO. 2007. *The Global Occupational Health Network Newsletter: elimination of silicosis* [Online]. Available: [http://www.who.int/occupational\\_health/publications/newsletter/gohnet12e.pdf](http://www.who.int/occupational_health/publications/newsletter/gohnet12e.pdf) [Accessed August 6 2013].
- WIESSNER, J. H., MANDEL, N. S., SOHNLE, P. G. & MANDEL, G. S. 1989. Effect of particle size on quartz-induced hemolysis and on lung inflammation and fibrosis. *Exp Lung Res*, 15, 801-12.
- WINTER, M., BEER, H. D., HORNUNG, V., KRAMER, U., SCHINS, R. P. & FORSTER, I. 2011. Activation of the inflammasome by amorphous silica and TiO<sub>2</sub> nanoparticles in murine dendritic cells. *Nanotoxicology*, 5, 326-40.
- WITTMACK, K. 2011. Novel dose metric for apparent cytotoxicity effects generated by in vitro cell exposure to silica nanoparticles. *Chem Res Toxicol*, 24, 150-8.

It doesn't matter  
The length of the journey  
But the resolve in the pursuit  
And the worth of the accomplishment